

## KAON DECAY STUDIES AT CERN SPS IN THE LAST DECADES

*A. Seccucci*<sup>1</sup>, *E. Goudzovski*<sup>2,3</sup>, *V. Kekelidze*<sup>3</sup>,  
*D. Madigozhin*<sup>3,\*</sup>, *I. Potrebenikov*<sup>3</sup>

<sup>1</sup> CERN, Geneva

<sup>2</sup> School of Physics and Astronomy, University of Birmingham, United Kingdom

<sup>3</sup> Joint Institute for Nuclear Research, Dubna

INTRODUCTION	1052
FUNDAMENTAL SYMMETRIES AND THEIR VIOLATIONS	1056
LOW-ENERGY QCD	1063
STANDARD MODEL AND POSSIBLE EXTENSIONS	1081
CONCLUSIONS	1087
REFERENCES	1087

---

\*E-mail: madigo@sunse.jinr.ru

## KAON DECAY STUDIES AT CERN SPS IN THE LAST DECADES

*A. Ceccucci*<sup>1</sup>, *E. Goudzovski*<sup>2,3</sup>, *V. Kekelidze*<sup>3</sup>,  
*D. Madigozhin*<sup>3,\*</sup>, *I. Potrebenikov*<sup>3</sup>

<sup>1</sup> CERN, Geneva

<sup>2</sup> School of Physics and Astronomy, University of Birmingham, United Kingdom

<sup>3</sup> Joint Institute for Nuclear Research, Dubna

This review summarizes the kaon experimental results obtained in the last 15 years on the basis of data collected at the CERN SPS with the participation of JINR physicists. These results contribute essentially to the Standard Model checks and search for its extension, fundamental symmetry violations and low-energy strong interactions theory development. A progress in the experimental technique and prospects for the future results are also discussed.

В обзоре представлены экспериментальные результаты по физике каонных распадов, полученные в последние 15 лет на основе данных, зарегистрированных на ускорителе SPS в ЦЕРН при участии физиков ОИЯИ. Эти результаты вносят существенный вклад в проверку Стандартной модели и поиск возможных выходов за ее пределы, в исследование нарушения фундаментальных симметрий и в разработку теории сильных взаимодействий при низких энергиях. Также обсуждается прогресс в экспериментальной технике и перспективы получения важных результатов в будущем.

PACS: 13.20.Eb; 13.25.ES

### INTRODUCTION

The physical results discussed here have been obtained on the basis of an experimental setup initially built for the NA48 experiment [1]. At the next stages the beamline and detectors have been somewhat modified in order to solve a series of new physical problems in the experiments NA48/1 [2] and NA48/2 [3]. For the 2007 run (so-called NA62  $R_K$  phase) this setup has been used in the new modification for the rare decay studies, which have solved both

---

\*E-mail: madigo@sunse.jinr.ru

the important physical problem [4] and the series of R&D tasks for the next-generation experiment NA62 [5], aimed at the super-rare decay  $K^+ \rightarrow \pi^+ \bar{\nu} \nu$  branching measurement.

**Detectors.** The detector part of the setup (Fig. 1) was not essentially modified due to its universality, but the beamline has been rebuilt considerably, especially for the transition from the neutral beams (NA48, NA48/1) to the charged ones (NA48/2, NA62  $R_K$  phase).

Charged particles were measured by the magnetic spectrometer composed of four drift chambers (DCH1–DCH4) filled with helium and a dipole magnet inducing a transverse momentum-kick of 265 MeV/c for the case of neutral beams. The spectrometer spatial resolution was 96  $\mu\text{m}$ , and its momentum resolution in this case was  $\sigma_p/p = ((0.48 \oplus 0.009)p)\%$ , where momentum  $p$  is in GeV/c. For the case of charged beams (NA48/2) the dipole magnet field was weakened (the transversal kick was 120 MeV/c) in order to diminish the charged beams deviation, and as a consequence the momentum resolution was larger:  $\sigma_p/p = ((1.02 \oplus 0.044)p)\%$ . The average efficiency per plane was 99.5%, with a radial uniformity better than 0.2%. The spectrometer was followed by the scintillator hodoscope. Fast logic was combining the strip signals for use in the different triggers.

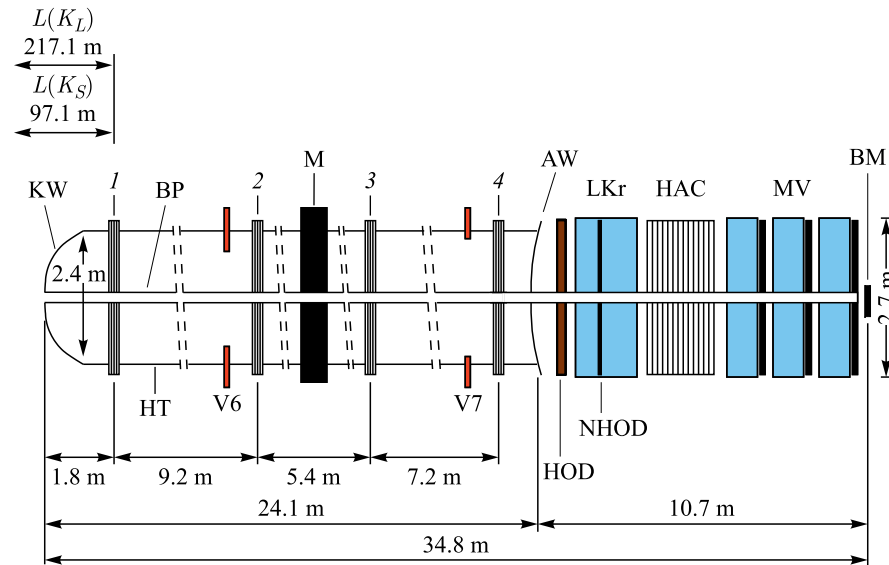


Fig. 1. NA48 detector setup (from [6]). KW — Kevlar window; BP — vacuum beam pipe; 1–4 — spectrometer drift chambers; HT — helium tank; V6, V7 — the last veto counters; M — spectrometer magnet; AW — aluminium window; HOD — charged particles hodoscope; NHOD — neutral component hodoscope; LKr — liquid krypton calorimeter; HAC — hadron calorimeter; MV — muon veto; BM — beam monitor

A liquid krypton calorimeter (LKr) was placed downstream of the hodoscope. It was 27 radiation lengths long and fully contained electromagnetic showers with energies up to 100 GeV. Transverse position of isolated shower was measured with a spatial resolution  $\sigma_x = \sigma_y = (0.42/\sqrt{E} \oplus 0.06)$  cm. Energy resolution for photons and electrons was  $\sigma_E/E = (3.2/\sqrt{E} \oplus 9.0/E \oplus 0.42)\%$  ( $E$  is a photon energy in units of GeV). LKr was segmented into about 13000 cells (each with  $2 \times 2$  cm cross section) and was used to reconstruct gamma quanta, electrons and positrons. Photon showers in the range 3–100 GeV were typically used for the analysis in order to avoid the low-energy nonlinearity. For most of analyses the electromagnetic shower position was required to be more than 15 cm away from the beam axis, more than 11 cm away from the outer edges of the calorimeter and more than 2 cm away from a defective calorimeter channel ( $\approx 0.4\%$  of the channels).

LKr was also used, together with the iron-scintillator hadron calorimeter, to measure the total deposited energy for triggering purposes. Muon veto counters (used to identify muons) were placed at the end of the beamline.

An aluminium beam pipe of 16 cm outer diameter and 1.1 mm thickness was traversing all the detector elements, providing the path in vacuum for beam particles and for the muons from the beam  $\pi^\pm$  decays (in the case of charged beams). At the beginning of NA48 data taking period, a carbon-fiber-reinforced polymer pipe has been used for this purpose, but its accidental destruction in 2000 has caused a costly repairment of drift chambers damaged by the implosion of helium into vacuum volume.

**Neutral Beams.** The  $K_L$  and  $K_S$  beams (Fig. 2) designed for the neutral kaon decays asymmetry measurements were produced in two different targets by protons from the same CERN SPS beam.

The primary proton beam from the CERN SPS accelerator ( $\approx 2.4 \cdot 10^{12}$  protons per pulse) impinged on the  $K_L$  target with an incidence angle of 2.4 mrad relative to the  $K_L$  beam axes. Then charged particles were removed from the outgoing beam by means of bending magnets. The fiducial decay volume was starting 126 m downstream of the target, where the beam was dominated by  $K_L$ ,  $\gamma$ , and neutrons.

The primary protons not interacting in the  $K_L$  target were directed onto the bent monocrystal of silicon. A small fraction of them was deviated in order to produce a collimated beam of  $\approx 5 \cdot 10^7$  ppp, which was then directed to the  $K_S$  target, located 72 mm above the  $K_L$  beam axis and 6 m upstream of the fiducial region. Two-pion decays from this beam come almost exclusively from  $K_S$  decays.

The tagging station (Tagger) was located on the  $K_S$  proton beam after the bent crystal. It consisted of two ladders of 12 scintillator strips each, covering the beam horizontally and vertically.

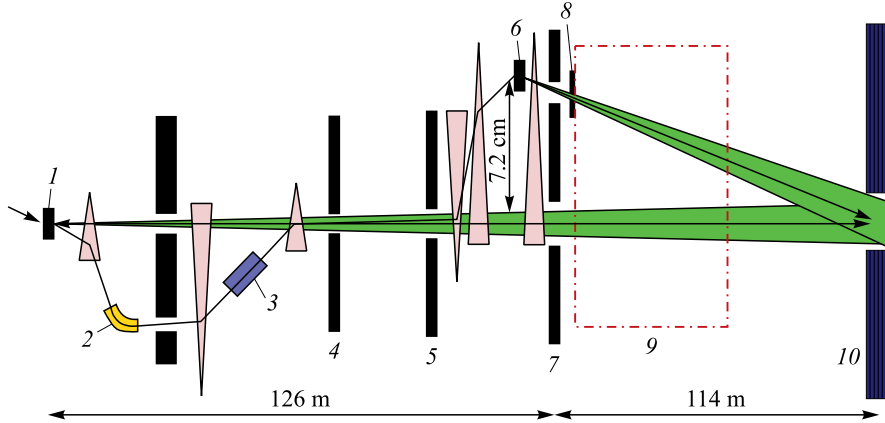


Fig. 2. NA48 synchronous  $K_L$  and  $K_S$  beams (not to scale, from [6]). 1 —  $K_L$  target; 2 — bent crystal; 3 —  $K_S$  tagger; 4 — defining collimator; 5 — cleaning collimator; 6 —  $K_S$  target; 7 — last collimator; 8 — early  $K_S$  decays veto (AKS); 9 — decay volume; 10 — NA48 detector setup

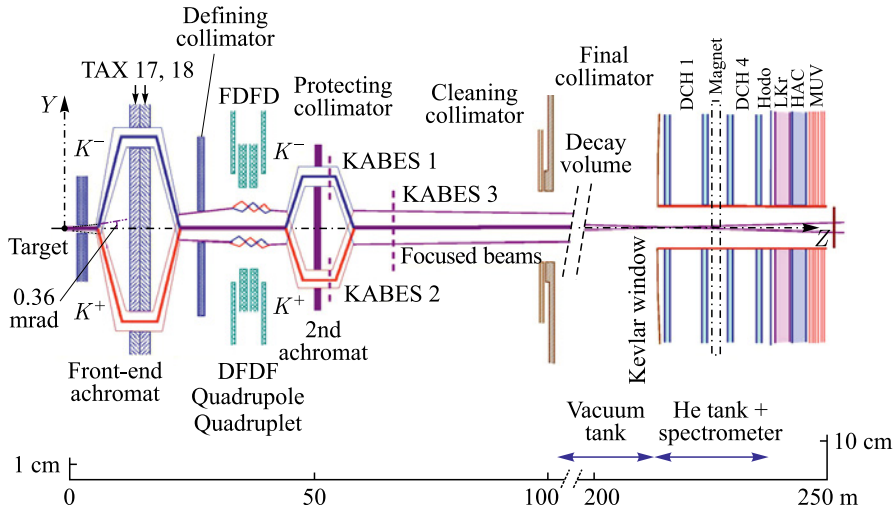


Fig. 3. NA48/2 charged beams (from [7]). TAX 17, 18 — collimators; DFDF — focusing quadrupoles; KABES 1–3 — beam spectrometer stations; DCH 1–4 — drift chambers; Hodo — hodoscope; LKr — electromagnetic calorimeter; HAC — hadron calorimeter; MUV — muon veto. The vertical scales for the beam and the detector regions are different

The beginning of the  $K_S$  decay region was defined by the anticounter (AKS), located at the exit of the  $K_S$  collimator.

**Charged Beams.** The beamline of the NA48/2 experiment was specifically designed to measure charge asymmetries in  $K^\pm \rightarrow 3\pi$  decays [7, 8]. Two simultaneous  $K^+$  and  $K^-$  beams were produced by 400 GeV/c protons on a beryllium target (Fig. 3). Particles of opposite charge with a central momentum of 60 GeV/c and a momentum band of  $\pm 3.8\%$  (rms) (74 GeV/c  $\pm 1.9\%$  for NA62  $R_K$  phase in 2007) were selected symmetrically by the system of magnets and collimators which separates vertically the two beams and recombines them again on the same axis.

Both beams of about 1 cm width were following almost the same path in the decay volume contained in the 114-m-long vacuum tank. The beams were dominated by  $\pi^\pm$ , the kaon component was about 6%. The  $K^+/K^-$  flux ratio was about 1.8.

## 1. FUNDAMENTAL SYMMETRIES AND THEIR VIOLATIONS

Fundamental symmetries, as well as their violations, always attract a special interest, as they reflect most general properties of our world. A considerable contribution to their understanding has been provided by kaon experiments performed at CERN.

**1.1. Extraction of the CP Violation Parameter  $|\eta^{+-}|$ .** Decay  $K_L \rightarrow \pi^+\pi^-$  was the first CP-violating phenomenon discovered as early as 1964 by Christenson, Cronin, Fitch, and Turlay (BNL) [9]. The measurements of this decay width defines an available precision of the indirect CP-violation parameter absolute value

$$|\eta^{+-}| = \sqrt{\frac{\Gamma(K_L \rightarrow \pi^+\pi^-)}{\Gamma(K_S \rightarrow \pi^+\pi^-)}} = \sqrt{\frac{\tau(K_S)\text{BR}(K_L \rightarrow \pi^+\pi^-)}{\tau(K_L)\text{BR}(K_S \rightarrow \pi^+\pi^-)}}. \quad (1)$$

In 2007, the NA48 collaboration presented a new precise measurement of the ratio of these decay rates  $\Gamma(K_L \rightarrow \pi^+\pi^-)/\Gamma(K_L \rightarrow \pi^\pm e^\mp \nu) = (4.835 \pm 0.022_{\text{stat}} \pm 0.016_{\text{syst}}) \cdot 10^{-3}$ . The analysis was based on the data taken during a dedicated run in 1999 by the NA48 experiment (see below Subsec. 1.2).

From this result the branching ratio of the CP-violating decay  $K_L \rightarrow \pi^+\pi^-$  and the CP-violating parameter  $|\eta^{+-}|$  have been calculated. Excluding the CP-conserving direct photon emission component  $K_L \rightarrow \pi^+\pi^-\gamma$ , the following final results have been obtained:  $\text{BR}(K_L \rightarrow \pi^+\pi^-) = (1.941 \pm 0.019) \cdot 10^{-3}$  and  $|\eta^{+-}| = (2.223 \pm 0.012) \cdot 10^{-3}$  [10].

These results were in contradiction with the PDG values published in 2004 [11]  $\text{BR}(K_L \rightarrow \pi^+\pi^-) = (2.090 \pm 0.025) \cdot 10^{-3}$  and  $|\eta^{+-}| = (2.288 \pm 0.014) \cdot 10^{-3}$ ,

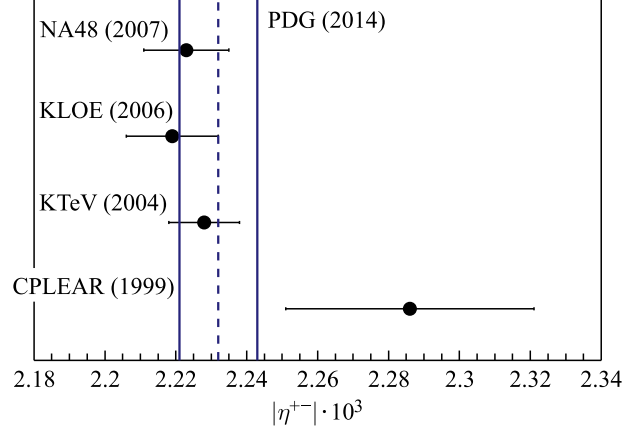


Fig. 4. Comparison of the NA48  $|\eta^{+-}|$  result [10] with the most recent other experimental results [12–14] and with the last PDG fit output [15]

but there was a good agreement with the most recent results of KTeV [13]  $\text{BR}(K_L \rightarrow \pi^+\pi^-) = (1.975 \pm 0.012) \cdot 10^{-3}$ ,  $|\eta^{+-}| = (2.228 \pm 0.010) \cdot 10^{-3}$  and KLOE [14]  $\text{BR}(K_L \rightarrow \pi^+\pi^-) = (1.963 \pm 0.021) \cdot 10^{-3}$ ,  $|\eta^{+-}| = (2.219 \pm 0.013) \cdot 10^{-3}$  (see Fig. 4).

The current PDG value [15] of  $\Gamma(K_L \rightarrow \pi^+\pi^-)/\Gamma(K_L \rightarrow \pi^\pm e^\mp \nu) = (4.849 \pm 0.020) \cdot 10^{-3}$  is mainly defined by the NA48 result [10] as well as by the last KTeV measurement [13].

**1.2. Direct CP Violation in Neutral Kaon Decays.** The effect discovered in 1964 is caused by the mixing of states with a different CP parity leading to the transitions between states during the relatively slow evolution of wave functions. It cannot affect the very short initial phase of the Universe emergence. So for the explanation of the predominance of matter over antimatter it was very important to obtain the proofs of existence of another CP-violating mechanism — *direct* violation right in the weak decay process.

As the indirect CP violation is caused only by the mixing of two CP states, it does not distinguish properties of the final states apart from their CP parity. In particular, indirect CP violation conserves the equality between two ratios:

$$\eta^{+-} = \frac{\langle \pi^+\pi^- | H | K_L \rangle}{\langle \pi^+\pi^- | H | K_S \rangle}; \quad \eta^{00} = \frac{\langle \pi^0\pi^0 | H | K_L \rangle}{\langle \pi^0\pi^0 | H | K_S \rangle}. \quad \text{Any violation of the equation}$$

$\eta^{+-} = \eta^{00}$  is a signature of nonmixing contribution to CP violation. In particular, the deviation of the double ratio

$$R = \frac{|\eta^{00}|^2}{|\eta^{+-}|^2} = \frac{\Gamma(K_L \rightarrow \pi^0\pi^0) \Gamma(K_S \rightarrow \pi^+\pi^-)}{\Gamma(K_S \rightarrow \pi^0\pi^0) \Gamma(K_L \rightarrow \pi^+\pi^-)} \quad (2)$$

from 1 may happen only due to the properties of the direct process of decay, and it is called a *direct* CP violation.

Due to the isotopic symmetry of two-pion final states, it is convenient to express the difference between  $K^0 \rightarrow \pi^+\pi^-$  and  $K^0 \rightarrow \pi^0\pi^0$  amplitudes in terms of special parameter  $\epsilon'$  in such a way that  $\eta^{+-} \approx \epsilon + \epsilon'$ ;  $\eta^{00} \approx \epsilon - 2\epsilon'$ , where  $\epsilon$  is the above parameter of indirect CP violation in kaon decays. Then one can write the relation

$$R \approx \frac{1 - 2 \left( \frac{\epsilon'^*}{\epsilon^*} + \frac{\epsilon'}{\epsilon} \right)}{1 + \left( \frac{\epsilon'^*}{\epsilon^*} + \frac{\epsilon'}{\epsilon} \right)} = \frac{1 - 4\text{Re} \left( \frac{\epsilon'}{\epsilon} \right)}{1 + 2\text{Re} \left( \frac{\epsilon'}{\epsilon} \right)} \approx 1 - 6\text{Re} \left( \frac{\epsilon'}{\epsilon} \right) \quad (3)$$

that may be used in order to measure the direct CP-violation intensity.

In the NA48 experiment [6,16], four decay modes entering (2) were collected simultaneously and in the same decay region, which minimizes the sensitivity of measurement to the variations in beam intensity and detection efficiency.  $K_L$  and  $K_S$  decays were provided by two almost collinear beams with similar momentum spectra, converging to the center of the main detector.  $K_L$  decays were weighted by the function of their proper lifetime in order to make the  $K_L$  decay distribution very similar to that of  $K_S$ . To be insensitive to the small beam momentum spectra differences, the analysis has been performed in bins of kaon energy.

In such a way, the acceptances almost cancel in the double ratio  $R$ , and only small remaining effects of the beam geometries have been corrected using Monte Carlo simulation.  $K_S$  decays are distinguished from  $K_L$  ones by a coincidence between the decay time and the time of protons producing the  $K_S$  beam. The measured double ratio is sensitive only to the differences in misidentification probabilities between the two decay modes.

*1.2.1. Event Reconstruction and Selection.*  $K \rightarrow \pi^0\pi^0$  decays were triggered requiring LKr energy deposit  $> 50$  GeV, a center of energy to the beam axis distance smaller than 25 cm, and a decay vertex less than  $5K_S$  lifetimes from the beginning of the decay volume. Four showers from the  $\pi^0\pi^0$  decay were within  $\pm 5$  ns of their average time. Event was rejected if there was an additional cluster of energy above 1.5 GeV and within  $\pm 3$  ns of the kaon decay candidate (in order to reduce the background from  $K_L \rightarrow 3\pi^0$  decays).

The distance  $D$  from the decay vertex to LKr was computed as  $D = \sqrt{\sum_j \sum_{i < j} E_i E_j ((x_i - x_j)^2 + (y_i - y_j)^2)} / m_K$ . Here  $E_i, x_i, y_i$  are the energy and position of the  $i$ th cluster. The average resolution on  $D$  was about 55 cm, and the resolution on the kaon energy was  $\approx 0.5\%$ . The invariant masses  $m_1$  and  $m_2$  of the two photon pairs were computed using  $D$  and then compared to the nominal  $\pi^0$  mass ( $m_{\pi^0}$ ) using the variable  $\chi^2 = \left[ \frac{(m_1 + m_2)/2 - m_{\pi^0}}{\sigma_+} \right]^2 +$

$\left[\frac{(m_1 - m_2)/2}{\sigma_-}\right]^2$ . Here  $\sigma_+$  and  $\sigma_-$  are the corresponding resolutions parameterized from the data as a function of the lowest photon energy. The minimal  $\chi^2$  photons pairing was kept for each candidate and a cut  $\chi^2 < 13.5$  was applied.

The  $\pi^+\pi^-$  decays were triggered using the scintillator hodoscope and a fast vertex reconstruction. A vertex position was calculated offline for each pair of tracks with opposite charge. The longitudinal vertex position resolution was about 50 cm, whereas the transverse resolution was around 2 mm. Since the beams were separated vertically by about 6 cm, an identification of the beam by the vertex position was applicable for the  $\pi^+\pi^-$  decays, while it was impossible for the  $\pi^0\pi^0$  ones. The tracks with momenta  $> 10$  GeV/c and not closer than 12 cm to the center of each chamber were accepted. The tracks closest approach for the vertex was required to be less than 3 cm. The tracks were required to be within the acceptance of LKr calorimeter and muon veto system.

The kaon energy was computed from the opening angle  $\theta$  of the two tracks and from the ratio of their momenta  $p_1$  and  $p_2$ , assuming  $K \rightarrow \pi^+\pi^-$  decay:  $E_K = \sqrt{\frac{\rho}{\theta^2}(m_K^2 - \rho m_\pi^2)}$ , where  $\rho = \frac{p_1}{p_2} + \frac{p_2}{p_1} + 2$ . In order to reject  $\Lambda \rightarrow p\pi^-$  decays, a cut was applied to the asymmetry  $A = |p_1 - p_2|/|p_1 + p_2|$ :  $A < \min(0.62, 1.08 - 0.0052 \times E_K)$ , where  $E_K$  is in GeV.

In order to suppress the background from semileptonic  $K_L$  decays, events with a muon veto hits near the track impact point as well as events with  $E_{\text{OP}} = E_{\text{LKr}}/p_{\text{DCh}} > 0.8$  (for one of the tracks) were rejected. Here  $p_{\text{DCh}}$  is a momentum of a track, and  $E_{\text{LKr}}$  is the energy of the LKr cluster, associated with the track.

The reconstructed kaon mass  $m_{\pi\pi}$  resolution was typically 2.5 MeV/c<sup>2</sup>. An energy-dependent cut at  $\pm 3\sigma_m$  was applied at the reconstructed mass value. The variable  $p'_T$  is defined as the kaon momentum component orthogonal to the line joining the production target and the impact point of the kaon on the first drift chamber plane. It was used to reduce further semileptonic decays background by means of the cut  $p'_T < 2 \cdot 10^{-4}$  GeV<sup>2</sup>/c<sup>2</sup>.

A decay was recognized as the  $K_S$  one if a coincidence was found within a  $\pm 2$  ns interval between the event time and a proton time measured by the Tagger. The tagging inefficiency  $(1.12 \pm 0.03) \cdot 10^{-4}$ , as well as the accidental mistagging probability  $(8.115 \pm 0.010) \cdot 10^{-2}$ , was directly measured in the  $\pi^+\pi^-$  mode. The difference of these probabilities between the  $\pi^0\pi^0$  and  $\pi^+\pi^-$  cases is calculated using the  $3\pi^0$  decays from  $K_L$  beam, as well as with the side tagging time windows technique.

*1.2.2. Corrections and Systematic Uncertainties.* A small inefficiency of the  $\pi^0\pi^0$  trigger is found to be  $K_S-K_L$  symmetric and no correction to  $R$  needs to be applied. For the  $\pi^+\pi^-$  case the correction was estimated and applied.

The kaon proper time used to count events is chosen to be  $0 < \tau < 3.5\tau_S$ , where  $\tau = 0$  is defined at the position of the AKS counter and  $\tau_S$  is  $K_S$  mean lifetime. For  $K_L$  events, the proper time cut was applied on reconstructed  $\tau$ , while for  $K_S$  events the cut at  $\tau = 0$  was applied using the AKS. The correction for the veto inefficiency difference between  $\pi^0\pi^0$  and  $\pi^+\pi^-$  cases has been estimated and implemented.

The background to the  $\pi^0\pi^0$  mode comes uniquely from  $K_L \rightarrow 3\pi^0$  decays. It was estimated from the  $K_L$  and  $K_S$  distributions of  $\chi^2$  using the Monte Carlo simulation to take into account the non-Gaussian tails in the calorimeter resolution.

The residual  $K_{e3}$  and  $K_{\mu3}$  backgrounds in  $\pi^+\pi^-$  mode were estimated by defining two control regions in the  $m_{\pi\pi} - p'_T$  plane, populated by the two kinds of  $\pi^+\pi^-$  background events with a different ratio.

In the  $K_L$  beam the  $p'_T$  cut (applied only in the  $\pi^+\pi^-$  mode) was stronger than the extrapolated kaon impact point radius cut (the last one is almost symmetrical between the  $\pi^+\pi^-$  and  $\pi^0\pi^0$  modes). It leads to the excess of the collimator scattered events in the  $\pi^0\pi^0$  mode that is taken into account by means of corresponding correction.

The  $K_S$  and  $K_L$  acceptances are made very similar in both modes by weighting  $K_L$  events according to their proper decay time. A small difference remains due to the differences in the beam sizes and directions. This residual correction is computed using a large-statistics Monte Carlo simulation.

The LKr absolute energy scale is checked using the data taken during special runs with a  $\pi^-$  beam striking two thin targets located near the beginning and the end of the fiducial decay region, producing  $\pi^0$  and  $\eta$  with the known decay positions.

Nonlinearities in the energy response are studied using special runs data and  $K_{e3}$  decays, where the electron energy is measured in calorimeter as well as in the drift chamber. The uniformity of the calorimeter response over its surface is optimized using  $K_{e3}$  decays and special runs data. The uncertainties due to the photons positions error and non-Gaussian tails in the energy response were also taken into account.

The uncertainty from the  $\pi^+\pi^-$  decays reconstruction takes into account the possible detector geometry deviations simulated by means of dedicated Monte Carlo code.

The overlap of accidental activity with a good event in the detectors may result in the net event loss effect in the reconstruction or the selection. This effect is cancelled with a good precision in double ratio  $R$  due to the simultaneous collection of data in the four channels and due to the very similar illumination of the detector by the  $K_L$  and  $K_S$  beams.

The possible residual effect can be separated into the two components. The first one (intensity difference effect) is given by  $\Delta R = \Delta\lambda \times \Delta I/I$ , where  $\Delta\lambda$  is the difference between the mean losses in  $\pi^+\pi^-$  and  $\pi^0\pi^0$  modes, and  $\Delta I/I$

is the difference in the mean  $K_L$  beam (the main source of accidental decays) intensity as seen by  $K_L$  and  $K_S$  events. The second component of the accidental effect (illumination difference) has been estimated from the overlay samples, computing separately the losses for  $K_S$  and  $K_L$  events. It has been performed using both data and Monte Carlo original events.

*1.2.3. Result.* The final NA48 result, obtained on the basis of 1997, 1998, 1999, and 2001 runs [16], after the recalculation of double ratio  $R$  to the direct CP-violation parameter (3) is the following:

$$\operatorname{Re}\left(\frac{\epsilon'}{\epsilon}\right) = (14.7 \pm 2.2) \cdot 10^{-4}. \quad (4)$$

This measurement of NA48 is one of the most precise ones (see Fig. 5). Together with the KTeV collaboration final result [17]  $\operatorname{Re}(\epsilon'/\epsilon) = (19.2 \pm 2.1) \cdot 10^{-4}$  and earlier measurements of E731 [18]  $(7.4 \pm 6.0) \cdot 10^{-4}$  and NA31 [19]  $(23.0 \pm 6.5) \cdot 10^{-4}$ , it defines the current knowledge on the direct CP-violation size in two-pion decays of neutral kaons.

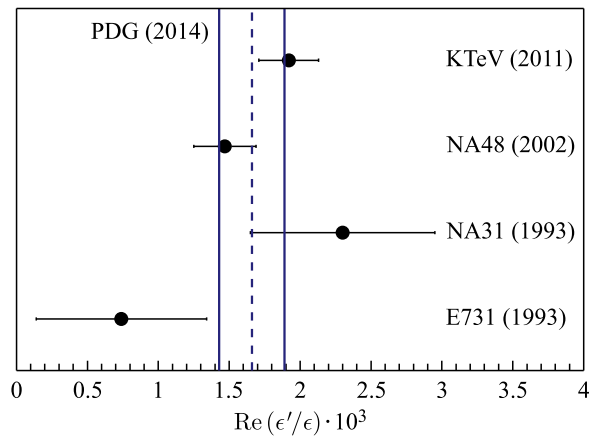


Fig. 5. Comparison of the NA48 final result [16] with other experimental results [17–19] and with the current PDG fit output [15]

**1.3. Search for Direct CP Violation in Charged Kaon Decays.** In kaon physics, besides the direct CP violation in two-pion decays of neutral kaons, a promising complementary observable may be an asymmetry between  $K^+$  and  $K^-$  decays to three pions.

The  $K^\pm \rightarrow 3\pi$  matrix element can be parameterized by a polynomial expansion in two Lorentz-invariant variables  $U$  and  $V$ :

$$|M|^2 \propto 1 + gU + hU^2 + kV^2 + \dots, \quad (5)$$

where  $|h|, |k| \ll |g|$  are the slope parameters. Here  $U = (s_3 - s_0)/m_{\pi^+}^2$ ,  $V = (s_2 - s_1)/m_{\pi^+}^2$  and  $s_i = (P_K - P_i)^2$ ,  $i = 1, 2, 3$ ;  $s_0 = (m_{K^+}^2 + 2m_{\pi^0}^2 + m_{\pi^+}^2)/3$ . Here  $P_i$  are the  $i$ th pion four-momenta and  $i = 3$  is assigned to the odd pion (other two pions have the same charge).

The parameter of direct CP violation for 3-pion decays of charged kaons is usually defined as  $A_G = (g^+ - g^-)/(g^+ + g^-)$ , where  $g^+$  is the linear coefficient in (5) for  $K^+$  and  $g^-$  — for  $K^-$ . Deviation of  $A_g$  from zero would be a clear indication of the direct CP violation.

The NA48/2 experiment at the CERN SPS was designed to search for direct CP violation in the decays of charged kaons into three pions, and collected data in 2003 and 2004. In order to reach a high accuracy in the measurement of the charge asymmetry parameter  $A_g$ , the highest possible level of charge symmetry between  $K^+$  and  $K^-$  was a main requirement in the choice of beam and strategy of data taking and analysis.

Charged beams for this experiment are described in Introduction. Frequent inversion of the magnetic field polarities in all the beamline elements provides a high level of intrinsic cancellation of the possible systematic effects in the beamline.

In order to minimize the effect of beam and detector asymmetries, the ratio  $R_4(u)$  has been used, defined as a product of four  $N^+(u)/N^-(u) \propto (1 + g^+U + hU^2)/(1 + g^-U + hU^2)$  ratios obtained with different polarities of beamline and polarities of spectrometer.

The *quadruple ratio*  $R_4(u)$  method complements the procedure of magnet polarity reversal. It allows a three-fold cancellation of systematic biases: beamline biases cancel between  $K^+$  and  $K^-$  samples in which the beams follow the same path; the effect of local nonuniformities of the detector cancels between  $K^+$  and  $K^-$  samples in which charged pions illuminate the same parts of the detectors; and as a consequence of using simultaneous  $K^+$  and  $K^-$  beams, time-dependent charge asymmetries cancels between  $K^+$  and  $K^-$  samples.

In total,  $3.11 \cdot 10^9 K^\pm \rightarrow 3\pi^\pm$  and  $9.13 \cdot 10^7 K^\pm \rightarrow \pi^\pm\pi^0\pi^0$  decays have been selected for analysis. Final results for the combined 2003 and 2004 data sets are [8]

$$A_g^c = (-1.5 \pm 1.5_{\text{stat}} \pm 0.9_{\text{trig}} \pm 1.3_{\text{syst}}) \cdot 10^{-4},$$

$$A_g^n = (1.8 \pm 1.7_{\text{stat}} \pm 0.6_{\text{syst}}) \cdot 10^{-4},$$

correspondingly for  $K^\pm \rightarrow 3\pi^\pm$  and  $K^\pm \rightarrow \pi^\pm\pi^0\pi^0$  decay modes. The results are one order of magnitude more precise than previous measurements and are consistent with the predictions of the SM, in particular, with the next-to-leading order ChPT calculation [20] ( $A_g^c = (-1.4 \pm 1.2) \cdot 10^{-5}$ ,  $A_g^n = (1.1 \pm 0.7) \cdot 10^{-5}$ ).

Current PDG values ( $A_g^c = (-1.5 \pm 1.5_{\text{stat}} \pm 1.6_{\text{syst}}) \cdot 10^{-4}$ ,  $A_g^n = (1.8 \pm 1.8) \cdot 10^{-4}$ ) [15] are defined mainly by the above NA48/2 results. The only

preceding result that is also used currently for PDG average,  $A_g^n = (2 \pm 18_{\text{stat}} \pm 5_{\text{syst}}) \cdot 10^{-4}$ , is published in 2005 [21].

Selected data sample of  $K^\pm \rightarrow 3\pi^\pm$  events has also been used for the measurement of the Dalitz plot parameters entering into (5). The following slope values have been obtained [22]:  $g = (-21.134 \pm 0.017)\%$ ,  $h = (1.848 \pm 0.040)\%$ ,  $k = (-0.463 \pm 0.014)\%$ . An order of magnitude precision improvement has been achieved, and this was the first measurement of nonzero value of quadratic slope parameter  $h$ . The measured slopes are in good agreement with the next-to-leading order computation [20]. Current PDG values of these slopes [15] are defined by the NA48/2 result, as the earlier measurements made in the seventies are based on much smaller statistics.

## 2. LOW-ENERGY QCD

**2.1. Pion Scattering in the Final State of  $K^\pm \rightarrow \pi^\pm \pi^0 \pi^0$  Decay.** The S-wave  $\pi\pi$  scattering lengths (multiplied by  $m_{\pi^\pm}$ ) for states with isospin  $I = 0$  ( $a_0^0$ ) and isospin  $I = 2$  ( $a_2^0$ ) are the most important parameters for the low-energy scattering amplitudes calculation. In the framework of Chiral Perturbation Theory (ChPT) the length  $a_0^0$  is connected with the size of chiral condensate and is predicted to have a value of  $a_0^0 = 0.220 \pm 0.005$ , while  $a_2^0 = -0.0444 \pm 0.0010$  [23].

During the analysis of NA48/2 collaboration 2003 data, a sharp change of the slope in the  $\pi^0\pi^0$  invariant mass ( $M_{00}$ ) distribution for  $K^\pm \rightarrow \pi^\pm \pi^0 \pi^0$  decays has been observed near the point of  $M_{00} = 2m_+$ , where  $m_+$  is the  $\pi^\pm$  mass [24].

The existence of this threshold anomaly as a result of the charge exchange scattering process  $\pi^+\pi^- \rightarrow \pi^0\pi^0$  in  $K^\pm \rightarrow \pi^\pm \pi^+ \pi^-$  decay was first predicted in 1961 [25]. But in the absence of experimental verification this early theoretical article has not attracted attention of physicists.

A first interpretation of the effect experimentally observed by NA48/2 in terms of  $\pi\pi$  rescattering in the final state has been made by N. Cabibbo [26], and then a second-order calculation [27] has provided the collaboration with a formula suitable for the experimental data fit. Another theoretical approach, based on the effective fields model, has been developed in [28,29] with another set of parameters for data distributions approximation. In both approaches the isospin symmetry-breaking correction was applied in the formulae connecting  $a_0^0$  and  $a_2^0$  to the five  $\pi\pi \rightarrow \pi\pi$  rescattering amplitudes with different charges of the pions.

The study of cusp effect is based on the data collected in 2003 and 2004 by the NA48/2 experiment. Nearly  $60 \cdot 10^6$   $K^\pm \rightarrow \pi^\pm \pi^0 \pi^0$  events were selected using the electromagnetic calorimeter data to reconstruct the photons from  $\pi^0$  decays and the magnetic spectrometer for charged pion tracks measurement (Fig. 6).

Matrix elements formulae from [27], as well as from [28,29], were used in order to fit the experimental  $M_{00}^2$  distribution taking into account the acceptance

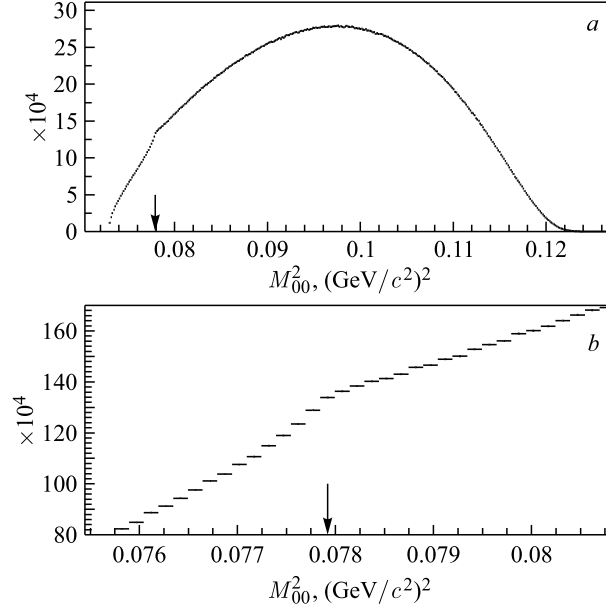


Fig. 6. *a*) Distribution of  $M_{00}^2$ , the square of the  $\pi^0\pi^0$  invariant mass; *b*) a narrow region of distribution centred at  $M_{00}^2 = (2m_+)^2$  (from [30])

and resolution effects calculated by means of Monte Carlo simulation. Differences between the fit results obtained with the two theoretical formulations are taken into account as theoretical errors of the scattering lengths measurement.

The following results for  $\pi\pi$  scattering lengths have been obtained [30]:

$$\begin{aligned} (a_0^0 - a_0^2)m_+ &= 0.2571 \pm 0.0048_{\text{stat}} \pm 0.0025_{\text{syst}} \pm 0.0014_{\text{ext}}, \\ a_0^2m_+ &= -0.024 \pm 0.013_{\text{stat}} \pm 0.009_{\text{syst}} \pm 0.002_{\text{ext}}. \end{aligned}$$

In addition to the statistical, systematic, and external errors, a theoretical uncertainty is found to be 0.0088(3.4%) for  $(a_0^0 - a_0^2)m_+$  and 0.015(62%) for  $a_0^2m_+$ .

From the measurement of pionium lifetime by the DIRAC experiment at the CERN PS [31], a value of  $|a_0^0 - a_0^2|m_+ = 0.264_{-0.020}^{+0.033}$  was deduced which agrees with NA48/2 result. Previous determinations of the  $\pi\pi$  scattering lengths have also relied on the measurement of  $K^\pm \rightarrow \pi^+\pi^-e^\pm\nu_e$  ( $K_{e4}$ ) decay. Figure 7 compares the cusp fit results with the results from the analysis of a large sample of  $K_{e4}$  decays, also collected by the NA48/2 collaboration [30] (see Subsec. 2.2).

One can use the theoretical connection between two scattering lengths [23] in order to extract  $a_0^0 - a_0^2$  with a better precision. With the ChPT constraint applied, the result is  $(a_0^0 - a_0^2)m_+ = 0.2633 \pm 0.0024_{\text{stat}} \pm 0.0014_{\text{syst}} \pm 0.0019_{\text{ext}}$ . Theoretical uncertainty affecting the value of  $a_0^0 - a_0^2$  is estimated to be  $\pm 2\%$  ( $\pm 0.0053$ ).

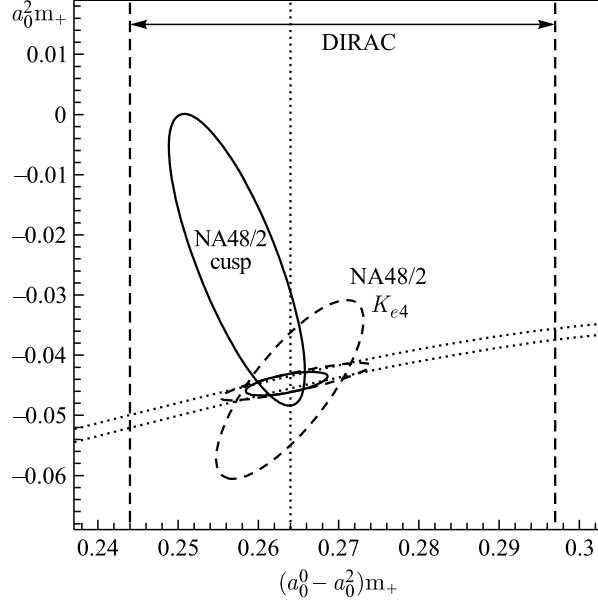


Fig. 7. 68% confidence level ellipses of the NA48/2 cusp analysis results (small solid line ellipse: fit with the ChPT constraint; large solid line ellipse: fit using  $a_0^0 - a_0^2$  and  $a_0^2$  as independent parameters) and from  $K_{e4}$  decay analysis [30] (dashed line ellipses). Vertical lines: DIRAC result [31]. ChPT constraint is shown between the dotted curves. From [30]

The 68% confidence level ellipses corresponding to the results with ChPT constraint are also shown in Fig. 7, together with a fit to the  $K_{e4}$  data which uses the same ChPT constraint.

On the basis of the same  $K^\pm \rightarrow \pi^\pm \pi^0 \pi^0$  decay analysis, a new empirical parameterization of this decay Dalitz plot has been proposed and fitted to experimental data [32]. The square of the matrix element can be written as

$$\frac{d|M|^2}{dUdV} \propto \left[ 1 + \frac{gU}{2} + \frac{hU^2}{2} + \frac{kV^2}{2} + a(U_t - U)^q H(U_t - U) + b(U - U_t)^q H(U - U_t) \right]^2 (1 + pw\delta(U - U_t)),$$

where  $H$  is the Heaviside step function, while  $U, V$  are defined in Subsec. 1.3. The constant  $w$  is equal to  $0.00015 (\text{GeV}/c^2)^2$  and  $U_t = (4m_{\pi^+}^2 - s_0)/m_{\pi^+}^2$ .

Near the cusp point  $U = U_t$  this approximation is only valid if the  $s_3$  distribution is averaged over bins which are wider than the width of the peak expected from  $\pi^+ \pi^-$  bound states and other electromagnetic effects [33], all decaying to  $\pi^0 \pi^0$ . This electromagnetic peak is much narrower than the bin width  $w$  used here, which is of the order of the experimental resolution.

The following parameter values for this empirical parameterization are extracted from the data analysis:

$$\begin{aligned}
g &= 0.672 \pm 0.001_{\text{stat}} \pm 0.011_{\text{syst}}, \\
h &= -0.027 \pm 0.001_{\text{stat}} \pm 0.011_{\text{syst}}, \\
k &= 0.0081 \pm 0.0002_{\text{stat}} \pm 0.0005_{\text{syst}}, \\
a &= -0.130 \pm 0.003_{\text{stat}} \pm 0.007_{\text{syst}}, \\
b &= -0.038 \pm 0.003_{\text{stat}} \pm 0.009_{\text{syst}}, \\
p &= 0.07 \pm 0.01_{\text{stat}} \pm 0.03_{\text{syst}}, \\
q &= 0.45 \pm 0.02_{\text{stat}} \pm 0.05_{\text{syst}}.
\end{aligned}$$

**2.2.  $K_{e4}$  Decays and Pion Scattering.** *2.2.1.  $K_{e4}^{+-}$  Decay.* The kinematics of the  $K^\pm \rightarrow \pi^+\pi^-e^\pm\nu$  ( $K_{e4}^{+-}$ ) decay is described by means of the five Cabibbo–Maksymowicz variables [34]: the square of dipion invariant mass  $S_\pi$ , the square of dilepton invariant mass  $S_e$ , the angle  $\theta_\pi$  of the  $\pi^\pm$  flight in the dipion rest frame with respect to the flight direction of dipion in the kaon rest frame, the angle  $\theta_e$  of the  $e^\pm$  in the dilepton rest frame with respect to the flight direction of dilepton in the kaon rest frame, and the angle  $\phi$  between the dipion and dilepton planes in the kaon rest frame.

The decay amplitude is the product of the leptonic weak current and ( $V - A$ ) hadronic current, that can be described in terms of three ( $F, G, R$ ) axial-vector and one ( $H$ ) vector complex form factors (for  $K_{e4}$  decay the sensitivity of decay matrix element to  $R$  form factor is negligible due to the small mass of electron). These form factors may be developed in a partial wave expansion with respect to the variable  $\cos\theta_\pi$ :

$$\begin{aligned}
F &= F_s e^{i\delta_{fs}} + F_p e^{i\delta_{fp}} \cos\theta_\pi + F_d e^{i\delta_{fd}} \cos^2\theta_\pi + \dots, \\
G &= G_p e^{i\delta_{gp}} + G_d e^{i\delta_{gd}} \cos\theta_\pi + \dots, \\
H &= H_p e^{i\delta_{hp}} + H_d e^{i\delta_{hd}} \cos\theta_\pi + \dots
\end{aligned}$$

Limiting the expansion to S- and P-waves and considering a unique phase  $\delta_p$  for all P-wave form factors in the absence of CP-violating weak phases, one will obtain the decay probability that depends only on the form factor magnitudes  $F_s, F_p, G_p, H_p$ , a single phase  $\delta = \delta_s - \delta_p$  and kinematic variables.

The form factors can be developed in a series expansion of the dimensionless invariants  $q^2 = (S_\pi/4m_\pi^2) - 1$  and  $S_e/4m_\pi^2$  [35]. Two slope and one curvature terms are sufficient to describe the measured  $F_s$  form factor variation within the available statistics ( $F_s = f_s(1 + f'_s/f_s q^2 + f''_s/f_s q^4 + f'_e/f_s S_e/4m_\pi^2)$ ), while two terms are enough to describe the  $G_p$  form factor ( $G_p/f_s = g_p/f_s + g'_p/f_s q^2$ ), and two constants to describe the  $F_p$  and  $H_p$  form factors.

Normalized  $K_{e4}^{+-}$  hadronic form factors in the S- and P-wave and their variation with energy have been obtained from the study of 1.13 million decays with a low relative background (0.6%) collected in 2003–2004 [36].

Reconstructed events were distributed in  $10 \times 5 \times 5 \times 5 \times 12$  equally populated bins in the  $(S_\pi, S_e, \cos(\theta_\pi), \cos(\theta_e), \phi)$  space. Ten independent fits (one per  $S_\pi$  bin) of five parameters ( $F_p, G_p, H_p, \delta$ , and a normalization constant that absorbs  $F_s$ ) were performed in four-dimensional space using the acceptance and resolution information from Monte Carlo simulation. The value of the phase difference  $\delta$  was extracted from the measured asymmetry of  $\phi$  distribution as a function of  $S_\pi$ .

The phase shift measurements can be related to the  $\pi\pi$  scattering lengths using the analytical properties and crossing symmetry of amplitudes (Roy equations [37]). In such a way the new precise measurements have been performed for the scattering lengths with a correction for isospin breaking mass effects:

$$\begin{aligned} a_0^0 &= 0.2220 \pm 0.0128_{\text{stat}} \pm 0.0050_{\text{syst}} \pm 0.0037_{\text{th}}, \\ a_0^2 &= -0.0432 \pm 0.0086_{\text{stat}} \pm 0.0034_{\text{syst}} \pm 0.0028_{\text{th}}. \end{aligned}$$

Using constraints based on analyticity and chiral symmetry [23], a more precise value for  $a_0^0$  has been obtained:  $a_0^0 = 0.2206 \pm 0.0049_{\text{stat}} \pm 0.0018_{\text{syst}} \pm 0.0064_{\text{th}}$ .

Combining both  $K_{e4}$  and cusp results from the two independent NA48/2 analyses with different sensitivities and using the constraint from ChPT [23], most precise experimental values have been obtained [36]:

$$\begin{aligned} a_0^0 &= 0.2196 \pm 0.0028_{\text{stat}} \pm 0.0020_{\text{syst}}, \\ a_0^0 - a_0^2 &= 0.2640 \pm 0.0021_{\text{stat}} \pm 0.0015_{\text{syst}}, \end{aligned}$$

corresponding to  $a_0^2 = -0.0444 \pm 0.0007_{\text{stat}} \pm 0.0005_{\text{syst}} \pm 0.0008_{\text{ChPT}}$ .

These last values can be used to estimate the phase of the direct CP-violating parameter  $\epsilon'$ , giving  $\phi_{\epsilon'} = (42.3 \pm 0.4)$  deg at the  $M_{K^0}$  energy of pions [36].

The best preceding  $\pi\pi$  scattering lengths experimental result of BNL E865 collaboration [38] based on the  $K_{e4}$  analysis

$$\begin{aligned} a_0^0 &= 0.228 \pm 0.012_{\text{stat}} \pm 0.004_{\text{syst}}^{+0.012}_{-0.016_{\text{th}}}, \\ a_0^2 &= -0.0365 \pm 0.0023_{\text{stat}} \pm 0.0008_{\text{syst}}^{+0.0031}_{-0.0026_{\text{th}}} \end{aligned}$$

is in reasonable agreement with the above final NA48/2 values. As an example of earlier measurements of  $a_0^0$  one can consider the CERN S118 collaboration value [39] published in 1977:  $a_0^0 = 0.28 \pm 0.05$ .

The  $K_{e4}^{+-}$  normalized (divided by  $f_s$ ) form factor parameters have been obtained by NA48/2 concurrently with the phase difference between the S- and P-wave states. But the absolute values measurement of the form factor parameters requires a branching fraction value. The corresponding  $K_{e4}^{+-}$  branching fraction measurement of the NA48/2 experiment has been published in [41].

Events selection for this purpose was rather close to the phase difference analysis one [36], but it was somewhat improved and modified for the maximum similarity to the selection of normalization channel  $K^\pm \rightarrow \pi^+\pi^-\pi^\pm$  ( $K_{3\pi}^{+-}$ ).

A track with  $p > 2.75$  GeV and  $0.9 < E/p < 1.1$  was identified as  $e^\pm$ , while the track with  $p > 5$  GeV and  $E/p < 0.8$  was regarded as  $\pi^\pm$ . A dedicated linear discriminant variable based on shower properties has been applied to reject events with one misidentified pion.

$K_{e4}^{+-}$  candidates were selected among the vertices with a single  $e^\pm$  candidate and a pair of  $\pi^+\pi^-$ . To suppress  $K_{3\pi}^{+-}$  background, the vertex invariant mass  $M_{3\pi}$  in the  $\pi^+\pi^-\pi^\pm$  hypothesis and its transverse momentum  $p_t$  were required to be outside an ellipse centered at PDG kaon mass [42] and zero transverse momentum, with semi-axes of 20 and 35 MeV/c, respectively.

The square missing mass of  $K^\pm \rightarrow \pi^\pm X$  decay was required to be larger than  $0.04$  (GeV/c<sup>2</sup>)<sup>2</sup> in order to reject  $\pi^\pm\pi^0$  decays with a subsequent  $\pi^0 \rightarrow e^+e^-\gamma$  process. The invariant mass of any possible  $e^+e^-$  system was required to be more than  $0.03$  GeV/c<sup>2</sup> to suppress the photon conversions.

For  $K_{e4}^{+-}$  events, the reconstruction of the kaon momentum assuming a four-body decay with the undetected neutrino was implemented, and the solution closest to 60 GeV/c was assigned to kaon momentum. For the normalization channel  $K_{3\pi}^{+-}$  the vertex was required to be composed of three charged pions.  $M_{3\pi}$  and  $p_t$  were inside the ellipse with semi-axes 12 and 25 MeV/c, respectively.

Events with reconstructed kaon momentum between 54 and 66 GeV/c were kept for the further analysis. A total sample of about 1.1 million  $K_{e4}^{+-}$  candidates and about 19 million prescaled  $K_{3\pi}$  candidates were selected from the data recorded in 2003–2004.

There are two main background sources for the signal of  $K_{e4}^{+-}$ :  $K^\pm \rightarrow \pi^+\pi^-\pi^\pm$  decays with a subsequent  $\pi \rightarrow e\nu$  decay or a pion misidentified as an electron; and  $K^\pm \rightarrow \pi^0(\pi^0)\pi^\pm$  with a subsequent  $\pi^0 \rightarrow e^+e^-\gamma$  decay with undetected photons and an electron misidentified as a pion. The background contribution below 1% level has been reached.

A detailed GEANT3-based [43] Monte Carlo simulation was used to take into account full detector geometry, DCH alignment, local inefficiencies and beam properties. The resulting  $K_{e4}^{+-}$  branching fraction is found to be  $\text{BR}(K_{e4}^{+-}) = (4.257 \pm 0.004_{\text{stat}} \pm 0.016_{\text{syst}} \pm 0.031_{\text{ext}}) \cdot 10^{-5}$ , which is 3 times more precise than the PDG value available at that time [42]. External error, caused by the uncertainty of the normalization channel branching fraction, is dominant in the total error of the measurement.

The preceding results for this branching fraction, entering into the current PDG fit ( $(4.254 \pm 0.032) \cdot 10^{-5}$  [15]), are the S118 value  $(4.03 \pm 0.18) \cdot 10^{-5}$  [39] and the E865 one  $(4.11 \pm 0.01 \pm 0.11) \cdot 10^{-5}$  [40].

$K_{e4}^{+-}$  form factor results comparison. In the E865 fit  $f'_e = f_p = 0$  is assumed

	NA48/2 [36,41]	E865 [38]
$f_s$	$5.705 \pm 0.003_{\text{stat}} \pm 0.017_{\text{syst}} \pm 0.031_{\text{ext}}$	$5.75 \pm 0.02 \pm 0.08$
$f'_s$	$0.867 \pm 0.040_{\text{stat}} \pm 0.029_{\text{syst}} \pm 0.005_{\text{norm}}$	$1.06 \pm 0.10 \pm 0.40$
$f''_s$	$-0.416 \pm 0.040_{\text{stat}} \pm 0.034_{\text{syst}} \pm 0.003_{\text{norm}}$	$-0.59 \pm 0.12 \pm 0.40$
$f'_e$	$0.388 \pm 0.034_{\text{stat}} \pm 0.040_{\text{syst}} \pm 0.002_{\text{norm}}$	—
$f_p$	$-0.274 \pm 0.017_{\text{stat}} \pm 0.023_{\text{syst}} \pm 0.002_{\text{norm}}$	—
$g_p$	$4.952 \pm 0.057_{\text{stat}} \pm 0.057_{\text{syst}} \pm 0.031_{\text{norm}}$	$4.66 \pm 0.05 \pm 0.07$
$g'_p$	$0.508 \pm 0.097_{\text{stat}} \pm 0.074_{\text{syst}} \pm 0.003_{\text{norm}}$	$0.67 \pm 0.10 \pm 0.04$
$h_p$	$-2.271 \pm 0.086_{\text{stat}} \pm 0.046_{\text{syst}} \pm 0.014_{\text{norm}}$	$-2.95 \pm 0.19 \pm 0.20$

The measured branching fraction has been used to extract  $f_s$  normalization form factor, which completes the full description of hadronic form factor parameterization. For the comparison to the preceding result [38], see the table. Currently only NA48/2 result is used to define the PDG values of  $K_{e4}^{+-}$  normalized form factor parameters [15].

2.2.2.  $K_{e4}^{00}$  Decay. For the case of  $K^\pm \rightarrow \pi^0 \pi^0 e^\pm \nu$  ( $K_{e4}^{00}$ ) decay, due to the restrictions of symmetry, matrix element does not depend on  $\theta_\pi$  and  $\phi$  angles. It may be parameterized in terms of the only form factor  $F_s$ , that in general case depends on  $S_\pi$  and  $S_e$ .

The  $K_{e4}^{00}$  rate is measured relative to the  $K^\pm \rightarrow \pi^0 \pi^0 \pi^\pm$  ( $K_{3\pi}^{00}$ ) normalization channel. These two modes are collected using the same trigger and with similar event selections.

Events with at least four  $\gamma$ , detected by LKr, and at least one track, reconstructed from spectrometer data, were regarded as  $K_{e4}^{00}$  or  $K_{3\pi}^{00}$  candidates. Every combination of four reconstructed  $\gamma$ 's with energies  $E > 3$  GeV was considered as a possible pair of  $\pi^0$  decays. Reconstructed longitudinal positions  $Z_1$  and  $Z_2$  of both  $\pi^0 \rightarrow 2\gamma$  decay candidates were required to coincide within 500 cm, with their average position  $Z_n = (Z_1 + Z_2)/2$  in the fiducial volume 106 m long.

Decay longitudinal position  $Z_{\text{ch}}$ , assigned to the track, was defined by the closest distance approach between the track and the beam axis. Combined vertex, composed of four LKr clusters and one charged track with momentum  $p > 5$  GeV, was required to have the difference  $|Z_n - Z_{\text{ch}}|$  less than 800 cm. If several combinations satisfy the vertex criteria, the case of minimum  $\left(\frac{Z_1 - Z_2}{\sigma_n}\right)^2 + \left(\frac{Z_n - Z_{\text{ch}}}{\sigma_c}\right)^2$  has been chosen, where  $\sigma_n$  and  $\sigma_c$  are the  $Z_n$ -dependent widths of corresponding distributions.

A track was preliminarily identified as  $e^\pm$ , if it has an associated LKr cluster with  $E/p$  between 0.9 and 1.1, otherwise  $\pi^\pm$  was assumed at the first stage.

Further suppression of pions misidentified as electrons is obtained by means of discriminant variable which is a linear combination of  $E/p$ , shower width and energy weighted track-to-cluster distance at LKr front face.

$K_{e4}^{00}$  and  $K_{3\pi}^{00}$  decays were discriminated by means of elliptic cuts in the  $(M_{\pi^0\pi^0\pi^\pm}, p_t)$  plane, where  $M_{\pi^0\pi^0\pi^\pm}$  is the invariant mass of combined vertex in the  $K_{3\pi}^{00}$  hypothesis, and  $p_t$  is the transverse momentum. Elliptic cut separates about 94 million  $K_{3\pi}^{00}$  normalization events from about 65000  $K_{e4}^{00}$  candidates. Residual fake-electron background is about 0.65% of  $K_{e4}^{00}$  amount. Background from  $K_{3\pi}^{00}$  with the subsequent  $\pi^\pm \rightarrow e^\pm\nu$  is 0.12% of the signal, and the accidental-related background is about 0.23%. It gives in total 1% of background admixture.

For the case of  $K^\pm \rightarrow \pi^0\pi^0e^\pm\nu$  ( $K_{e4}^{00}$ ) decay, due to the presence of two identical particles in dipion, it cannot be in antisymmetric ( $l = 1$ ) state, so form factors cannot include P-terms. In the first approximation, only S-wave contributes, and the matrix element is parameterized in terms of the only form factor  $F_s$ , which may depend on  $S_\pi$  and  $S_e$ . Form factor  $F_s$  was extracted from the fit of events distribution on  $(S_e, S_\pi)$  plane, taking into account the acceptance, calculated from MC simulation.

The following empirical  $K_{e4}^{00}$  form factors parameterization has been proposed for the first time:

$$\frac{F_s}{f_s} = 1 + \left(\frac{f'_s}{f_s}\right) q^2 + \left(\frac{f''_s}{f_s}\right) q^4 + \left(\frac{f'_e}{f_s}\right) \frac{S_e}{4m_\pi^2} \quad \text{for } q^2 > 0,$$

$$\frac{F_s}{f_s} = 1 + d \sqrt{\left|\frac{q^2}{(1+q^2)}\right|} + \left(\frac{f'_e}{f_s}\right) \frac{S_e}{4m_\pi^2} \quad \text{for } q^2 < 0.$$

The results of the fit published in [44] are in good agreement with the above NA48/2  $K_{e4}^{+-}$  analysis:

$$\frac{f'_s}{f_s} = 0.149 \pm 0.033_{\text{stat}} \pm 0.014_{\text{syst}},$$

$$\frac{f''_s}{f_s} = -0.070 \pm 0.039_{\text{stat}} \pm 0.013_{\text{syst}},$$

$$\frac{f'_e}{f_s} = 0.113 \pm 0.022_{\text{stat}} \pm 0.007_{\text{syst}},$$

$$d = -0.256 \pm 0.049 \pm 0.016_{\text{syst}}.$$

Below the threshold of  $S_\pi = (2m_{\pi^\pm})^2$  the measured  $K_{e4}^{00}$  decay form factor shows some deficit of events with respect to the polynomial approximation, which is well described by the used empirical parameterization (Fig. 8). It looks similar to the cusp effect of  $\pi^+\pi^- \rightarrow \pi^0\pi^0$  rescattering in  $K^\pm \rightarrow \pi^0\pi^0\pi^\pm$  decay.

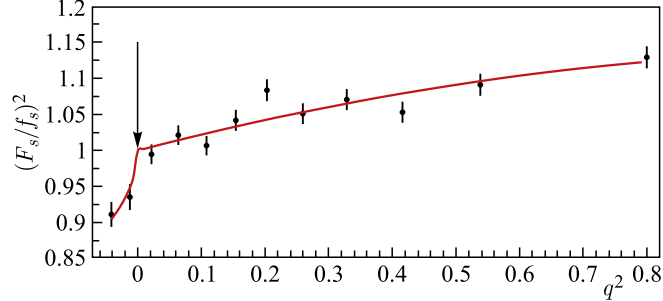


Fig. 8.  $K_{e4}^{00}$  normalized form factor squared as a function of  $q^2$ . The line corresponds to the adopted empirical fit. The arrow points to the  $2m_\pi$  threshold. From [44]

The obtained form factor was used to obtain the final result of branching fraction measurement [44]:  $\text{BR}(K_{e4}^{00}) = (2.552 \pm 0.010_{\text{stat}} \pm 0.010_{\text{syst}} \pm 0.032_{\text{ext}}) \times 10^{-5}$ . Systematic error includes the contributions from background, simulation statistical error, sensitivity to form factor, radiation correction, trigger efficiency and beam geometry. External error comes from uncertainty of normalization channel  $K_{3\pi}^{00}$  branching fraction.

This result is 10 times more precise than the last PDG value  $(2.2 \pm 0.4) \times 10^{-5}$  [15], still defined mainly by the early measurements [45] ( $\text{BR}(K_{e4}^{00}) = (2.54 \pm 0.89) \cdot 10^{-5}$ ) and [46] ( $\Gamma(K_{e4}^{00})/\Gamma(\pi^0 e^- \nu_e) = (4.2_{-0.9}^{+1.0}) \cdot 10^{-4}$ ).

**2.3.  $K_{l3}$  Decays Form Factors.** Semileptonic kaon decays  $K \rightarrow \pi l \nu$  offer the most precise determination of the CKM matrix element  $|V_{us}|$ . The hadronic matrix element of these decays is usually described in terms of two form factors (vector  $f_+(t)$  and scalar  $f_0(t)$  ones), both depending on  $t = (p_K - p_\pi)^2$ .

Since the measurement of the matrix element overall normalization is a separate experimental task with its specific systematic uncertainties, normalized decay form factors  $\bar{f}_{+,0}(t)$  are usually defined in such a way that  $\bar{f}_{+,0}(0) = 1$ . Historically, the first set of parameterizations for these functions was the quadratic one:

$$\bar{f}_{+,0}(t) = 1 + \lambda'_{+,0} \frac{t}{m_\pi^2} + \frac{1}{2} \lambda''_{+,0} \frac{t^2}{m_\pi^4}.$$

The NA48/2 experiment with the charged kaon beams provides a largest events statistics, collected in 2003 and 2004, for precision measurement of both  $K^\pm \rightarrow \pi^0 \mu^\pm \nu$  ( $K_{\mu 3}^\pm$ ) and  $K^\pm \rightarrow \pi^0 e^\pm \nu$  ( $K_{e 3}^\pm$ ) semileptonic decay form factors.

At least one track in spectrometer and two clusters in the electromagnetic calorimeter were required by the event selection procedure. The track had to be in the geometrical acceptance of the relevant detector elements (DCH, LKr, MUV).

For electron tracks a proper timing and a momentum  $p > 5 \text{ GeV}/c$  were required. For muons the momentum needed to be greater than  $10 \text{ GeV}/c$  to ensure proper efficiency of the MUV system. To identify the track as a muon, the

presence of associated hit in the MUV system and  $E/p < 0.2$  were necessary. Here  $E$  is the energy measured by LKr (in GeV) and  $p$  is the DCH track momentum (in GeV/c). For electrons a range of  $0.95 < E/p < 1.05$  and the absence of associated hit in the MUV system were required.

Two LKr clusters with energies  $E > 3$  GeV were regarded as a candidate to  $\pi^0$  decay, if both of them were well isolated from any track hitting the calorimeter, and both were in time with the selected charged track. An absolute value of missing mass squared of the reconstructed  $K_{l3}^\pm$  event with an undetected neutrino was required to be less than  $0.01$   $(\text{GeV}/c^2)^2$ .

For  $K_{\mu 3}^\pm$ , the background from  $K^\pm \rightarrow \pi^\pm \pi^0$  events with the subsequent  $\pi^\pm \rightarrow \mu^\pm \nu$  decay was suppressed by means of combined cut of the invariant mass  $m_{\pi^\pm \pi^0}$  (under  $\pi^\pm$  hypothesis) and  $\pi^0$  transverse momentum. Residual background contamination is 0.5%.

Another source of background is due to  $K^\pm \rightarrow \pi^\pm \pi^0 \pi^0$  events with the  $\pi^\pm$  decay and a lost  $\pi^0$ . The corresponding estimated contamination amounts to about 0.1%. It is a small contribution, but it introduces a slope in the Dalitz plot. So the corresponding correction has been applied at the final analysis stage.

For  $K_{e3}^\pm$ , only the background from  $K^\pm \rightarrow \pi^\pm \pi^0$  with  $\pi^\pm$  misidentified as electron significantly contributes to the signal. A cut in the transverse momentum of the event reduced this background to less than 0.1%.

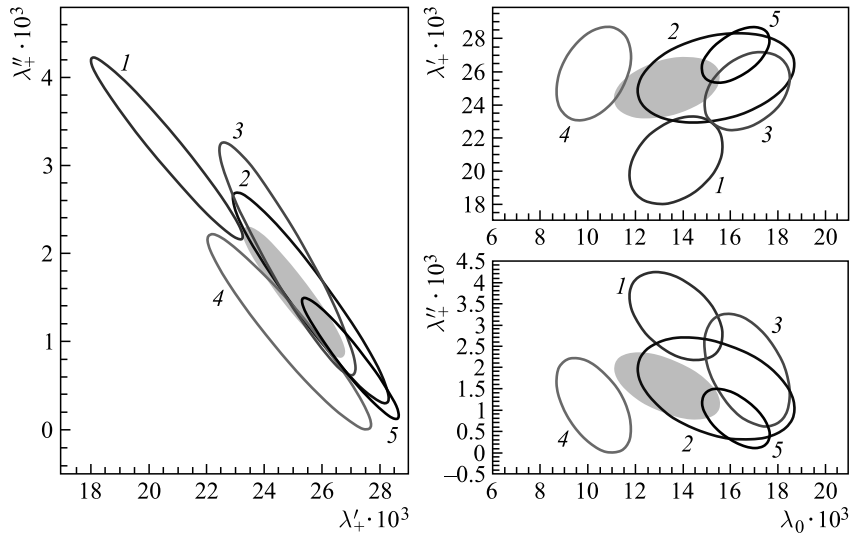


Fig. 9. 68% confidence level contours for the  $K_{l3}$  combined quadratic fit results (from [48]): 1 — KTeV ( $K^0$ , [49]); 2 — KLOE ( $K^0$ , [50]); 3 — Istra+ ( $K^-$ , [51,52]); 4 — NA48 ( $K^0$ , [53]); 5 — NA48/2 ( $K^\pm$ , preliminary result [48]). The FlaviaNet group fit results [54] are shown as gray areas. From [48]

As a result,  $2.5 \cdot 10^6 K_{\mu 3}^{\pm}$  and  $4.0 \cdot 10^6 K_{e 3}^{\pm}$  decays were selected. The reconstructed Dalitz plot was corrected for remaining background, detector acceptance (simulated by means of Monte Carlo program based on GEANT3 package [43]) and distortions induced by radiative effects. The radiative effects were simulated by using a special Monte Carlo generator developed by the KLOE collaboration [47]. To extract the form factors, a two-dimensional fit to the Dalitz plot density was performed in space of the lepton and pion energies in the kaon center of mass.

The  $K_{l3}$  quadratic parameterization fit combined results of recent experiments are shown in Fig.9. The 68% confidence level contours are plotted for both neutral  $K_{l3}^0$  (KLOE, KTeV, and NA48) and charged  $K_{l3}^{\pm}$  decays.

The preliminary NA48/2 results [48] are the first high-precision measurements done with both  $K^+$  and  $K^-$  mesons jointly. The obtained form factors are in agreement with the other measurements (except  $K_{\mu 3}^0$  one from NA48 [53]) and compatible with the FlaviaNet combined fit [54].

**2.4. Rare Kaon Decays.** The NA48 and NA48/2 data collected for their primary goals of CP-violation measurement also provide a large sample of precisely measured kaon decays of many rare modes. These data are still used in order to improve our knowledge about the strong interactions at low energies. As an example we will discuss here just a few recent analyses of the rare decays performed in the NA48/2 experiment.

*2.4.1.  $K^{\pm} \rightarrow \pi^{\pm} \pi^0 \gamma$  Decay.* The total amplitude of the  $K^{\pm} \rightarrow \pi^{\pm} \pi^0 \gamma$  decay consists of two terms: the inner bremsstrahlung (IB) associated with the  $K^{\pm} \rightarrow \pi^{\pm} \pi^0$  decay ( $K_{2\pi}^{\pm}$ ) and a photon emitted from the  $\pi^{\pm}$ , and the direct emission (DE) in which the photon is emitted from the weak vertex. The IB branching ratio could be evaluated from the QED corrections. It is suppressed because  $K_{2\pi}^{\pm}$  is suppressed by the  $\Delta I = 1/2$  rule, resulting in a relative enhancement of the DE contribution.

Direct photon emission can occur through both electric (E) and magnetic (M) dipole transitions. The E transition can interfere with the IB amplitude giving rise to an interference term (INT), which can have CP-violating contribution. In ChPT calculations DE arises only at the order of  $O(p^4)$  and cannot be evaluated in a model-independent way. The M part consists of two amplitudes: one reducible and another expected to be small.

An experimental measurement of both DE and INT terms allows the determination of both the E and M contributions. The properties of  $K^{\pm} \rightarrow \pi^{\pm} \pi^0 \gamma$  decay can be described in terms of two variables:  $T_{\pi}^*$  — kinetic energy of  $\pi^{\pm}$  in the kaon rest frame, and  $W^2 = (P_K \cdot P_{\gamma})(P_{\pi} \cdot P_{\gamma}) / (m_K m_{\pi})^2$ , where  $P_K$ ,  $P_{\pi}$ ,  $P_{\gamma}$  are 4-momenta of  $K^{\pm}$ ,  $\pi^{\pm}$  and  $\gamma$ , respectively.

The implemented selection criteria (see [55]) allowed one to select 600k  $K^{\pm} \rightarrow \pi^{\pm} \pi^0 \gamma$  decays in the range of  $0 < T_{\pi}^* < 80$  MeV with the background

level  $< 10^{-4}$ . The DE term is proportional to  $W^4$  and the INT term is proportional to  $W^2$ . This allows one to decouple two term contributions comparing the obtained  $W$  spectrum with the MC simulation and to measure the ratios [55]:

$$\begin{aligned} \text{Frac}_{\text{DE}}(0 < T_\pi^* < 80 \text{ MeV}) &= \frac{\text{BR}_{\text{DE}}}{\text{BR}_{\text{IB}}} = (3.32 \pm 0.15_{\text{stat}} \pm 0.14_{\text{syst}}) \cdot 10^{-2}, \\ \text{Frac}_{\text{INT}}(0 < T_\pi^* < 80 \text{ MeV}) &= \frac{\text{BR}_{\text{INT}}}{\text{BR}_{\text{IB}}} = (-2.35 \pm 0.35_{\text{stat}} \pm 0.39_{\text{syst}}) \cdot 10^{-2}. \end{aligned}$$

This is the first observation of an interference term (INT) in the  $K^\pm \rightarrow \pi^\pm \pi^0 \gamma$  decay.

In addition, an asymmetry of branching ratios has been measured:  $A_N = (N^+ - RN^-)/(N^+ + RN^-)$ , where  $N^+$  and  $N^-$  are the numbers of  $K^+ \rightarrow \pi^+ \pi^0 \gamma$  and  $K^- \rightarrow \pi^- \pi^0 \gamma$  decays, respectively, and  $R$  is the ratio of the numbers of  $K^+$  and  $K^-$  in the beam. This asymmetry, indicating a possible CP violation in decay, has been obtained to be less than  $1.5 \cdot 10^{-3}$  at the 90% C.L. A measured asymmetry of  $W$  spectra gives another upper limit for CP violation:  $A_W = (-0.6 \pm 1.0_{\text{stat}}) \cdot 10^{-3}$ . The current PDG value [15] of this experimental asymmetry  $(9 \pm 33) \cdot 10^{-3}$  is based on the late seventies' results  $(8 \pm 58) \cdot 10^{-3}$  [56] and  $(10 \pm 40) \cdot 10^{-3}$  [57].

**2.4.2.  $K^\pm \rightarrow \pi^\pm l^+ l^-$  Decays.** The FCNC processes  $K^\pm \rightarrow \pi^\pm l^+ l^-$  ( $l = e, \mu$ ) are induced at one-loop level in the Standard Model. Their decay rates are dominated by the long-distance contribution via one-photon exchange, and have been described by the Chiral Perturbation Theory (ChPT). Recent precise measurements of these decays based on the data collected by the NA48/2 experiment have been reported in the papers [58, 62].

The decay is supposed to proceed through single virtual photon exchange, resulting in a spectrum of the  $z = (M_{ee}/M_K)^2$  kinematic variable sensitive to the form factor  $W(z)$  [63]:

$$\frac{d\Gamma}{dz} = \frac{\alpha^2 M_K}{12\pi(4\pi)^4} \lambda^{3/2}(1, z, r_\pi^2) \sqrt{1 - 4\frac{r_l^2}{z}} \left(1 + 2\frac{r_e^2}{z}\right) |W(z)|^2, \quad (6)$$

where  $r_l = m_l/M_K$ ,  $r_\pi = m_\pi/M_K$ , and  $\lambda(a, b, c) = a^2 + b^2 + c^2 - 2ab - 2ac - 2bc$ . The following parameterizations of the form factor  $W(z)$  are considered in the NA48/2 analysis:

1. Linear:  $W(z) = G_F M_K^2 f_0 (1 + \delta z)$  with free parameters  $f_0$  and  $\delta$ .
2. Next-to-leading order ChPT [63]:  $W(z) = G_F M_K^2 (a_+ + b_+ z) + W^{\pi\pi}(z)$  with free parameters  $(a_+, b_+)$  and an explicitly calculated pion loop term  $W^{\pi\pi}(z)$ .
3. Combined framework of ChPT and large- $N_c$  QCD [64]: the form factor is parameterized as  $W(z) \equiv W(\tilde{w}, \beta, z)$  with free parameters  $(\tilde{w}, \beta)$ .

4. ChPT parameterization [65] involving meson form factors:  $W(z) \equiv W(M_a, M_\rho, z)$ . The resonance masses ( $M_a, M_\rho$ ) are treated as free parameters in the present analysis.

2.4.3.  $K^\pm \rightarrow \pi^\pm e^+ e^-$  Decay. The  $K^\pm \rightarrow \pi^\pm e^+ e^-$  decay rate is measured by NA48/2 relative to  $K^\pm \rightarrow \pi^\pm \pi_D^0$  normalization channel (where  $\pi_D^0 \rightarrow e^+ e^- \gamma$  is the Dalitz decay) [58]. A large part of the selection is common to signal and normalization modes. Three-track vertices were reconstructed by extrapolation of track segments from the spectrometer into the fiducial decay volume. The tracks measured momenta were in the range of  $5 < p < 50$  GeV/c. Track separations exceeded 2 cm in DCH1 plane to suppress  $\gamma$  conversions, and 15 cm in LKr front plane to minimize effects of shower overlaps. The three-track vertex was required to be composed of one  $\pi$  candidate ( $E/p < 0.85$ ) and a pair of oppositely charged  $e^\pm$  candidates ( $E/p > 0.95$ ). For the normalization channel an LKr cluster from  $\gamma$  with  $E > 3$  GeV was required additionally. The reconstructed kaon total momentum was accepted within the beam nominal range:  $54 < |\vec{p}_{\pi ee}| < 66$  GeV/c, while the transverse momentum with respect to the beam trajectory (measured using the concurrently acquired  $K^\pm \rightarrow 3\pi^\pm$ ) was less than  $0.5 \cdot 10^{-3}$  (GeV/c)<sup>2</sup>.

In the case of signal  $K^\pm \rightarrow \pi^\pm e^+ e^-$  mode, the  $\pi^\pm e^+ e^-$  invariant mass was required to be inside the range of  $470 < M_{\pi ee} < 505$  MeV/c<sup>2</sup>. The lower limit corresponds to an  $E_\gamma < 23.1$  MeV cutoff for the energy of a single directly undetectable soft IB photon. In order to avoid a large background from  $K^\pm \rightarrow \pi^\pm \pi_D^0$ , the signal decay was analyzed only in the region of  $z = (M_{ee}/M_K)^2 > 0.08$ , which leads to a loss of  $\sim 30\%$  of the signal sample. The reconstructed  $\pi^\pm e^+ e^-$  invariant mass spectrum is presented in Fig. 10, *a*. Background contamination is measured to be  $(1.0 \pm 0.1)\%$ .

For the  $K^\pm \rightarrow \pi^\pm \pi_D^0$  normalization mode candidates, an  $e^+ e^- \gamma$  invariant mass compatible with a  $\pi_D^0$  decay was required:  $|M_{ee\gamma} - M_{\pi^0}| < 10$  MeV/c<sup>2</sup>, as well as the reconstructed kaon invariant mass compatible with its expected value:  $475 < M_{\pi ee\gamma} < 510$  MeV/c<sup>2</sup>.

The Coulomb factor and radiative corrections are taken into account; they are crucial for the extrapolation of the branching ratio from the limited  $M_{\pi ee}$  signal region.

The  $z$  spectrum of the data events in the visible region  $z > 0.08$  are presented in Fig. 10, *b*. The values of  $d\Gamma_{\pi ee}/dz$  in the centre of each  $i$ -bin of  $z$  are computed as

$$\left(\frac{d\Gamma_{\pi ee}}{dz}\right)_i = \frac{N_i - N_i^B}{N_n} \frac{A_n(1 - \varepsilon_n)}{A_i(1 - \varepsilon_i)} \frac{1}{\Delta z_i} \frac{\hbar}{\tau_K} \text{BR}_n. \quad (7)$$

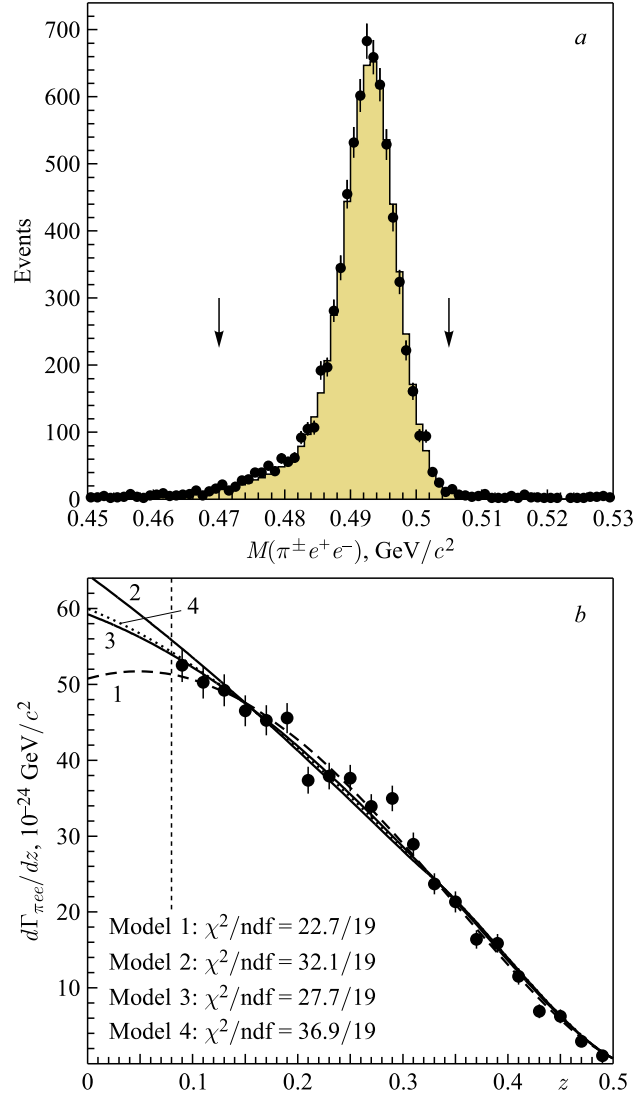


Fig. 10. *a*) Reconstructed spectrum of  $\pi^\pm e^+ e^-$  invariant mass: data (dots) and MC simulation (filled area). *b*)  $d\Gamma_{\pi ee}/dz$  and fit results according to the four considered models. From [58]

Here  $N_i$  and  $N_i^B$  are numbers of  $K^\pm \rightarrow \pi^\pm e^+ e^-$  candidates and background events in the  $i$ th bin;  $N_n$  is the number of the normalization channel  $K^\pm \rightarrow \pi^\pm \pi_D^0$  events (background subtracted);  $A_i$  and  $\varepsilon_i$  are geometrical acceptance and trigger

inefficiency in the  $i$ th bin for the signal sample (computed by MC simulation);  $A_n$  and  $\varepsilon_n$  are those for  $K^\pm \rightarrow \pi^\pm \pi_D^0$  events;  $\Delta z$  is the bin width set to 0.02. The external inputs are the kaon lifetime  $\tau_K$  and normalization branching ratios entering  $\text{BR}_n = \text{BR}(K^\pm \rightarrow \pi^\pm \pi^0) \cdot \text{BR}(\pi_D^0)$ .

The values of  $d\Gamma_{\pi ee}/dz$  and results of the fits to the four models are presented in Fig. 10. Each of the considered models provides a reasonable fit to the data. The differences between model-dependent branching fractions come from the region  $z < 0.08$ .

From a sample of 7253  $K^\pm \rightarrow \pi^\pm e^+ e^-$  decay candidates with 1.0% background contamination, the branching ratio in the full kinematic range, which includes a model-dependence uncertainty, has been measured to be  $\text{BR} = (3.11 \pm 0.04_{\text{stat}} \pm 0.05_{\text{syst}} \pm 0.08_{\text{ext}} \pm 0.07_{\text{model}}) \cdot 10^{-7}$ . It is in reasonable agreement (see Fig. 12) with the previous measurements:  $(2.7 \pm 0.5) \cdot 10^{-7}$  (Geneva–Saclay [59]),  $(2.75 \pm 0.23_{\text{stat}} \pm 0.13_{\text{syst}}) \cdot 10^{-7}$  (E777 [60]) and  $(2.94 \pm 0.05_{\text{stat}} \pm 0.13_{\text{syst}} \pm 0.05_{\text{model}}) \cdot 10^{-7}$  (E865 [61]).

The direct CP-violating charge asymmetry of decay rates has been measured for the first time:  $\Delta(K_{\pi ee}^\pm) = (\text{BR}^+ - \text{BR}^-)/(\text{BR}^+ + \text{BR}^-) = (-2.2 \pm 1.5_{\text{stat}} \pm 0.6_{\text{syst}}) \cdot 10^{-2}$ , corresponding to an upper limit of  $|\Delta(K_{\pi ee}^\pm)| < 2.1 \cdot 10^{-2}$  at 90% CL.

**2.4.4.  $K^\pm \rightarrow \pi^\pm \mu^+ \mu^-$  Decay.** The  $K^\pm \rightarrow \pi^\pm \mu^+ \mu^-$  decay ( $K_{\pi\mu\mu}$ ) rate has been measured by NA48/2 relative to  $K^\pm \rightarrow \pi^\pm \pi^+ \pi^-$  normalization channel ( $K_{3\pi}$ ) [62]. Charged tracks were selected with momenta  $> 10$  GeV/ $c$  to ensure high muon identification efficiency. One of the tracks was required to have  $E/p < 0.85$  and no in-time associated hits in MUV, which one could expect for charged pion. For  $K_{\pi\mu\mu}$  case both tracks were required to be compatible with muons ( $E/p < 0.2$  and associated hits in the first two planes of MUV), while for  $K_{3\pi}$  selection for these two tracks there was no particle identification requirements. In both cases the corresponding reconstructed kaon mass was selected within  $\pm 8$  MeV/ $c^2$  around PDG value (Fig. 11, *a*).

The values of  $d\Gamma_{\pi\mu\mu}/dz$  in small  $z$  bins have been extracted from data according to (7) with the corresponding normalization channel  $K^\pm \rightarrow \pi^\pm \pi^+ \pi^-$ . The effective  $z_i$  values, at which  $(d\Gamma_{\pi\mu\mu}/dz)_i$  are evaluated, are corrected for the distribution nonlinearity following [66]. The resulting distribution is plotted in Fig. 11, *b* together with the linear fit result. The fits to the other models are very similar and are not shown. The model-independent BR is evaluated by integration of the spectrum [64] normalized to the full  $K^\pm$  decay width  $\hbar/\tau_K$ .

From a sample of 3120  $K^\pm \rightarrow \pi^\pm \mu^+ \mu^-$  decay candidates with a  $(3.3 \pm 0.7)\%$  background contamination, the model-independent branching fraction has been measured to be  $\text{BR} = (9.62 \pm 0.21_{\text{stat}} \pm 0.11_{\text{syst}} \pm 0.07_{\text{ext}}) \cdot 10^{-8}$ , and the form factor that characterizes the decay has been evaluated in the framework of four models. The branching fraction result is in agreement with the previous results

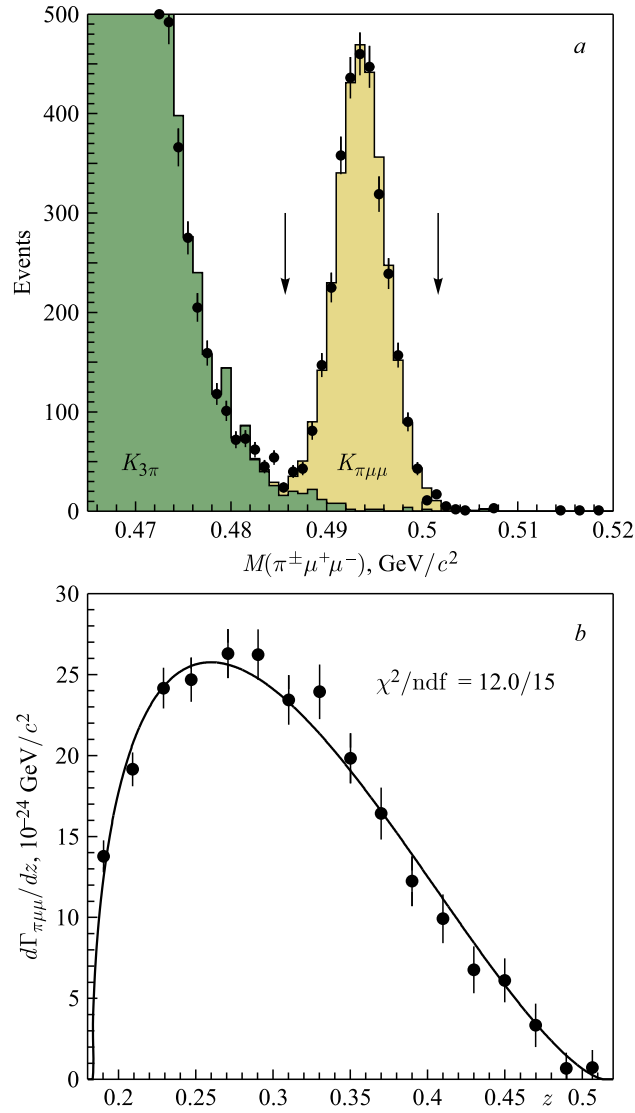


Fig. 11. *a*) Reconstructed spectrum of  $\pi^\pm\mu^+\mu^-$  invariant mass: data (dots),  $K^\pm \rightarrow \pi^\pm\mu^+\mu^-$  MC simulation and  $K^\pm \rightarrow 3\pi^\pm$  background estimate (filled areas). *b*)  $d\Gamma_{\pi\mu\mu}/dz$  and fit result with a linear form factor parameterization. From [62]

$(9.8 \pm 1.0 \pm 0.5) \cdot 10^{-8}$  (HyperCP [67]) and  $(9.22 \pm 0.6 \pm 0.49) \cdot 10^{-8}$  (E865 [68]), but disagrees with the earliest result  $(5.0 \pm 0.4 \pm 0.6 \pm 0.7) \cdot 10^{-8}$  (E787 [69]), see Fig. 12.

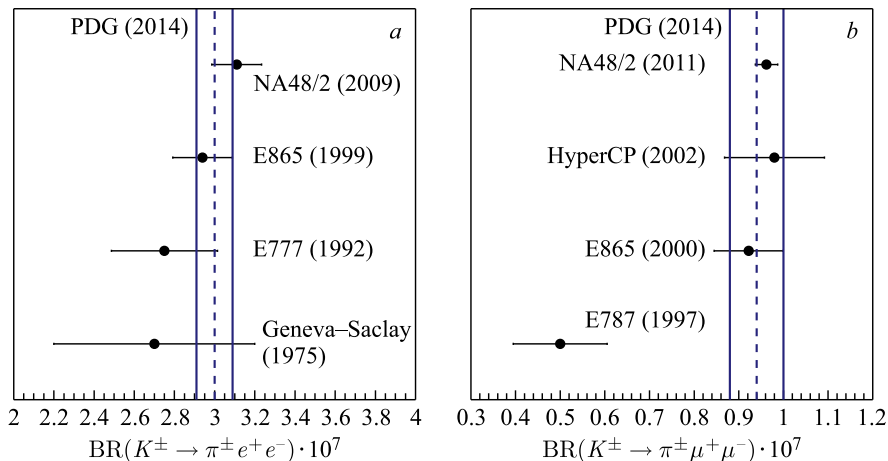


Fig. 12. *a*) Comparison of the NA48/2  $\text{BR}(K^\pm \rightarrow \pi^\pm e^+ e^-)$  result [58] with the other experimental results [59–61] and with the last PDG fit output [15]. *b*) Comparison of the NA48/2  $\text{BR}(K^\pm \rightarrow \pi^\pm \mu^+ \mu^-)$  result [62] with [69, 68, 67] and with the last PDG fit

Separate measurements of the BR for  $K^+$  and  $K^-$  decays allow the evaluation of the CP-violating charge asymmetry of the decay rate that has been measured to be  $(1.1 \pm 2.3)\%$ . It is an essential improvement in precision with respect to the previous measurement  $(-2 \pm 11 \pm 4)\%$  [67]. Apart from that, a 90% CL upper limit of 2.3% for the decay rate forward-backward asymmetry has been established by NA48/2 for the first time.

Also an upper limit of  $1.1 \cdot 10^{-9}$  for the branching fraction of the lepton-number-violating  $K^\pm \rightarrow \pi^\mp \mu^\pm \mu^\pm$  decay has been obtained. This is an improvement by almost a factor of 3 with respect to the best previous limit  $3 \cdot 10^{-9}$  [70].

**2.4.5.  $K^\pm \rightarrow \pi^\pm \gamma \gamma$  Decay.** In the ChPT framework, the  $K^\pm \rightarrow \pi^\pm \gamma \gamma$  decay receives two noninterfering contributions at lowest nontrivial order  $\mathcal{O}(p^4)$ : the pion and kaon *loop amplitude* depending on an unknown  $\mathcal{O}(1)$  constant  $\hat{c}$  representing the total contribution of the counterterms, and the *pole amplitude* [71].

New measurements of this decay have been performed using data collected during a 3-day special NA48/2 run in 2004 and a 3-month NA62 run in 2007. The  $K_{\pi\gamma\gamma}$  decay rate has been measured with respect to the normalization decay chain:  $K^\pm \rightarrow \pi^\pm \pi^0$  decay followed by  $\pi^0 \rightarrow \gamma\gamma$ .

For both signal and normalization modes, only one reconstructed charged particle track with the closest distance of approach (CDA) to beam axis less than 3.5 cm and with the momentum  $p$  between 8 and 50 GeV/ $c$  was required. The ratio of corresponding LKr cluster energy to the track momentum, measured by means of spectrometer, was  $E/p < 0.8$ . Two LKr clusters with energies

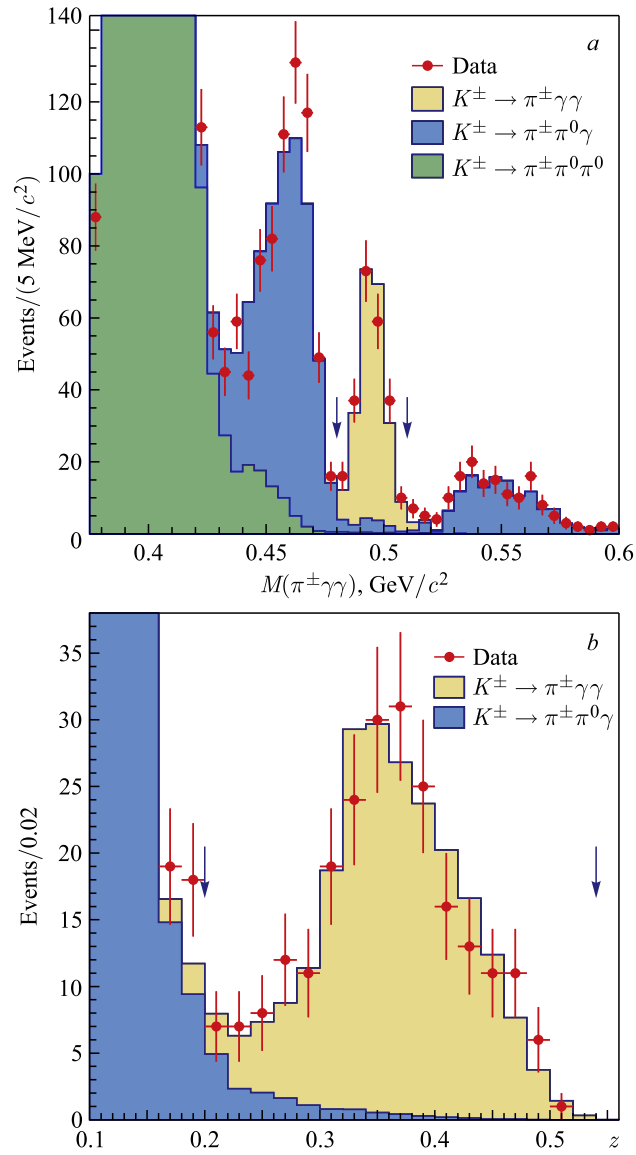


Fig. 13. *a*) NA62 ( $R_K$  phase) reconstructed spectrum of  $\pi^\pm\gamma\gamma$  invariant mass: data (dots), signal MC simulation and background estimate (filled areas). *b*) Reconstructed  $z = (m_{\gamma\gamma}/m_K)^2$  spectrum for selected  $K_{\pi\gamma\gamma}$  candidates compared to the simulated signal and background distributions. Signal region is indicated with vertical arrows. From [72]

$E > 3 \text{ GeV}/c$  in time with the track ( $\pm 15 \text{ ns}$ ), but separated by at least  $25 \text{ cm}$  from the track impact point on LKr front plane were considered as  $\gamma$  candidates. An energy-dependent upper limit was imposed on the cluster lateral width to suppress the contribution of cases with cluster merging.

Signal events are selected in the region of  $z = (m_{\gamma\gamma}/m_K)^2 > 0.2$  to reject the  $K^\pm \rightarrow \pi^\pm \pi^0$  background peaking at  $z = 0.075$  (see Fig. 13). For  $K_{2\pi}$  as a normalization channel,  $0.064 < z < 0.086$  was required. 149 (232) decays candidates are observed in the 2004 (2007) data set, with backgrounds contaminations of 10.4% (7.5%) from  $K^\pm \rightarrow \pi^\pm \pi^0(\pi^0)(\gamma)$  decays with merged photon clusters in the electromagnetic calorimeter.

The values of  $\hat{c}$  in the framework of the ChPT  $\mathcal{O}(p^4)$  and  $\mathcal{O}(p^6)$  parameterizations [73], as well as branching ratio, have been measured using likelihood fits to the data. The main systematic effect is due to the background uncertainty. Uncertainties related to trigger, particle identification, acceptance and accidental effects were found to be negligible. The final combined results based on 2004 and 2007 runs data [72, 74] are: for  $\mathcal{O}(p^4)$  fit,  $\hat{c} = 1.72 \pm 0.20_{\text{stat}} \pm 0.06_{\text{syst}}$ ; for  $\mathcal{O}(p^6)$  fit,  $\hat{c} = 1.86 \pm 0.23_{\text{stat}} \pm 0.11_{\text{syst}}$ ; for  $\mathcal{O}(p^6)$  fit, branching fraction  $\text{BR}(K_{\pi\gamma\gamma}) = (1.003 \pm 0.056) \cdot 10^{-6}$ . The model-independent branching ratio for  $z > 0.2$  is equal to  $(0.965 \pm 0.063) \cdot 10^{-6}$ . New results are in agreement with the earlier (based on 31 events) BNL E787 [75] ones:  $\hat{c} = 1.8 \pm 0.6$ , total  $\text{BR}(K_{\pi\gamma\gamma}) = (1.1 \pm 0.3_{\text{stat}} \pm 0.1_{\text{syst}} \pm 0.12_{\text{model}}) \cdot 10^{-6}$ .

### 3. STANDARD MODEL AND POSSIBLE EXTENSIONS

**3.1. Ratio of the Charged Kaon Leptonic Decay Rates.** In the Standard Model (SM) the decays of pseudoscalar mesons to light leptons are helicity suppressed. Although the SM predictions for the leptonic decay rates are limited by hadronic uncertainties, their specific ratios can be computed very precisely. In particular, the SM prediction for the ratio  $R_K = \Gamma(K_{e2})/\Gamma(K_{\mu 2})$  of kaon leptonic decay widths inclusive of internal bremsstrahlung (IB) radiation is [76]

$$R_K^{\text{SM}} = \left(\frac{m_e}{m_\mu}\right)^2 \left(\frac{m_K^2 - m_e^2}{m_K^2 - m_\mu^2}\right)^2 (1 + \delta R_{\text{QED}}) = (2.477 \pm 0.001) \cdot 10^{-5}, \quad (8)$$

where  $\delta R_{\text{QED}}$  is electromagnetic correction due to the IB and structure-dependent effects.

Within certain two Higgs doublet models (2HDM of type II), including the minimal supersymmetric model (MSSM),  $R_K$  is sensitive to lepton-flavour-violating (LFV) effects appearing at the one-loop level via the charged Higgs boson ( $H^\pm$ ) exchange representing a unique probe into mixing in the right-handed slepton sector [77–79].

A new experimental result for  $R_K$  based on the dedicated data collected in 2007 by the NA62 collaboration was published in 2013 [4]. The measure-

ment method is based on counting the numbers of reconstructed  $K_{e2}$  and  $K_{\mu2}$  candidates collected concurrently.  $R_K$  evaluation is performed independently in 10 bins of lepton momentum covering the range of 13–65 GeV/ $c$  for four statistically independent data samples (collected for two different detector configurations and two kaon charge signs). Acceptances were calculated by means of Monte Carlo simulation, but the particle identification, trigger and readout efficiencies were measured directly from the experimental data.

Due to the topological similarity of  $K_{e2}$  and  $K_{\mu2}$  decays, a large part of the selection conditions is common for both decay modes: (1) exactly one reconstructed positively charged particle compatible with that originating from a beam  $K$  decay; (2) its momentum  $13 < p < 65$  GeV/ $c$  (the lower limit is due to the 10 GeV LKr energy deposit trigger requirement); (3) extrapolated track impact points in subdetectors are within their geometrical acceptances; (4) no LKr energy deposition clusters with energy  $E > 2$  GeV not associated to the track, to suppress background from other kaon decays; (5) distance between the charged track and the nominal kaon beam axis  $CDA < 3$  cm, and decay vertex longitudinal position within the nominal decay volume.

Selection conditions for missing mass were dependent on lepton momentum and on the missing mass resolution for the specific decay mode. Particles with  $0.95 < E/p < 1.1$  ( $E/p < 0.85$ ) were identified as positrons (muons).

At high lepton momentum, the  $K_{\mu2}$  decay with a misidentified muon ( $E/p > 0.95$ ) is the largest background source. The dominant process leading to misidentification of the muon as a positron is a “catastrophic” bremsstrahlung in or in front of LKr leading to significant energy deposit in LKr. The muon misidentification probability  $P_{\mu e}$  has been measured as a function of momentum. To collect a muon sample free from the positron contamination, a  $9.2X_0$  thick lead (Pb) wall covering  $\approx 20\%$  of the geometric acceptance was installed approximately 1.2 m in front of the LKr calorimeter.

To evaluate the correction factor  $f_{\text{Pb}} = P_{\mu e}/P_{\mu e}^{\text{Pb}}$ , a dedicated MC simulation based on Geant4 (version 9.2) has been developed to describe the propagation of muons downstream of the last DCH, involving all electromagnetic processes including muon bremsstrahlung [80].

A fit to the measurements of  $R_K$  in the 10 lepton momentum bins (see Fig. 14) for four data samples collected in different experimental conditions has been performed, taking into account the bin-to-bin correlations between the systematic errors. The result is

$$R_K = (2.488 \pm 0.007_{\text{stat}} \pm 0.007_{\text{syst}}) \cdot 10^{-5}. \quad (9)$$

It is in agreement with the most precise previous measurement result of KLOE  $R_K = (2.493 \pm 0.025_{\text{stat}} \pm 0.019_{\text{syst}}) \cdot 10^{-5}$  [81]. Current PDG value  $2.488 \pm 0.009$  [15] is the average of these two results.

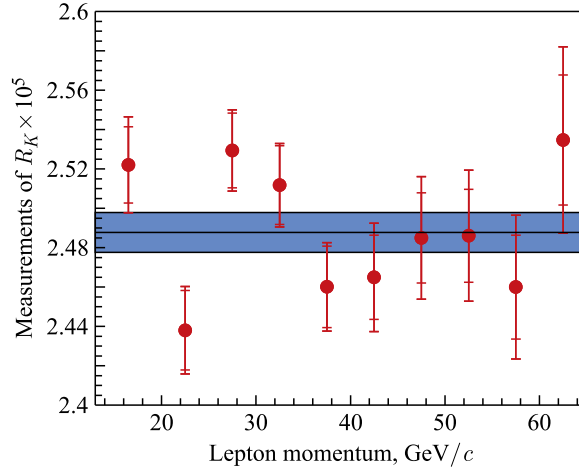


Fig. 14.  $R_K$  measurements in lepton momentum bins. From [4]

This measurement of lepton-flavour-violation parameter  $R_K$  is consistent with the SM expectation, and can be used to constrain multi-Higgs [77] and fourth-generation [82] new physics scenarios.

**3.2. Search for the Dark Photon.** Charged kaons represent a source of tagged neutral pion decays, mainly via  $K^\pm \rightarrow \pi^\pm \pi^0$  decay. Therefore, high-intensity kaon experiment provide opportunities for precision studies of  $\pi^0$  decay physics. The large sample of neutral pions produced and decaying in vacuum collected by NA48/2 allows for a high-sensitivity search for the dark photon (DP,  $A'$ ), a hypothetical gauge boson appearing in hidden sector of new physics models with an extra  $U(1)$  gauge symmetry.

Dark Photon (DP) is characterized by a priori unknown mass  $m_{A'}$  and mixing parameter  $\epsilon$  defining the interaction of DP with the visible sector. It may be registered via the chain of decays:  $K^\pm \rightarrow \pi^\pm \pi^0$ ,  $\pi^0 \rightarrow \gamma A'$ ,  $A' \rightarrow e^+ e^-$ , with three charged particles and a photon in the final state.

For kinematical and theoretical reasons, with a good precision one can expect  $\text{BR}(A' \rightarrow e^+ e^-) \approx 1$ . Its mean path in the NA48/2 conditions does not exceed 10 cm and can be neglected in the first approximation. So the three-track vertex topology can be used without significant acceptance loss. Dalitz decay  $\pi_D^0 \rightarrow e^+ e^- \gamma$  represents an irreducible background and determines the sensitivity.

In the NA48/2 experiment a dedicated two-level trigger was in operation to collect three-track decays with an efficiency of about 98%. A sample of about  $4.7 \cdot 10^6$  reconstructed  $\pi_D^0$  decay candidates in the  $e^+ e^-$  invariant mass range  $m_{ee} > 10 \text{ MeV}/c^2$  with a negligible extra background has been selected. The

candidates mainly originate from  $K^\pm \rightarrow \pi^\pm \pi_D^0$  decays ( $K_{2\pi D}$ ), with 0.15% coming from the  $K^\pm \rightarrow \pi_D^0 \mu^\pm \nu$  decays ( $K_{\mu 3D}$ ).

The reconstructed  $e^+e^-$  invariant mass ( $m_{ee}$ ) spectrum of the  $K_{2\pi D}$  candidates does not display any narrow peaks that would be a signature of a dark photon produced in  $\pi_D^0$  decay and decaying promptly to  $e^+e^-$ .

A search for the DP assuming different mass hypotheses with a variable mass step has been performed. In total, 398 DP mass hypotheses have been tested in the range  $10 < m_{ee} < 125 \text{ MeV}/c^2$ .

For all of them the statistical significance of DP signal  $S = (N_{\text{obs}} - N_{\text{exp}}) / \sqrt{(\delta N_{\text{obs}})^2 + (\delta N_{\text{exp}})^2}$  (where  $N_{\text{obs}}$  and  $N_{\text{exp}}$  are the observed and expected number of events, correspondingly) does not exceed 3.5, meaning that no significant signal is observed.

The upper limits at 90% CL on  $\text{BR}(\pi^0 \rightarrow \gamma A')$  as well as the upper limits on the mixing parameter  $\epsilon^2$  value calculated from these branching fraction limits for each of the mass hypotheses are published in [83].

In Fig. 15, the NA48/2 upper limits for  $\epsilon^2$  are shown together with the constraints from the SLAC E141 and FNAL E774 [84–86], KLOE [87], WASA [88], HADES [89], A1 [90], APEX [91], and BaBar [92] experiments. Also shown is the band where the discrepancy between the measured and calculated muon

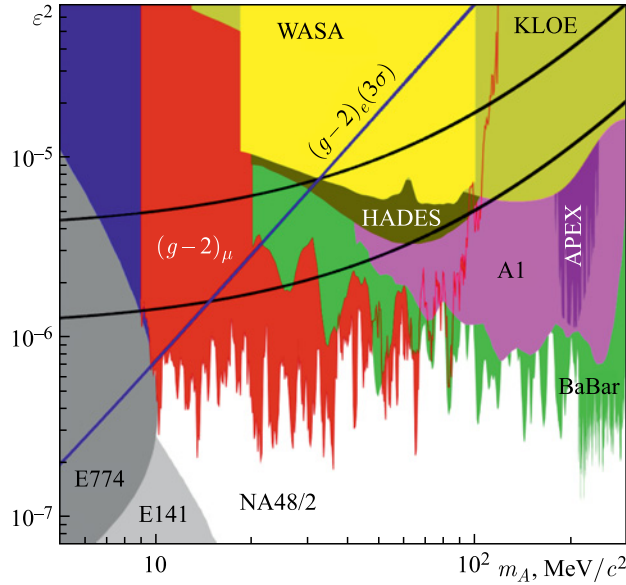


Fig. 15. Upper limits obtained by NA48/2 at 90% CL on the mixing parameter  $\epsilon^2$  versus dark photon mass, compared to other published exclusion limits (see text for references). From [83]

$(g - 2)$  values falls into the  $\pm 2\sigma$  range due to the dark photon contribution, as well as the region excluded by the electron  $(g - 2)$  measurement [93–95].

The region of dark photon mass  $m(A') < 10 \text{ MeV}/c^2$  is excluded at 90% CL by the electron beam dump experiments [86], while the lowest upper limits for  $m(A') > 60 \text{ MeV}/c^2$  are currently provided by the A1 [90], APEX [91], and BaBar [92], typically at the  $\epsilon^2$  order of magnitude of  $10^{-6}$ . The NA48/2 collaboration has established the upper limit below  $\epsilon^2 = 10^{-6}$  for the dark photon mass between 10 and 90  $\text{MeV}/c^2$ . This result represents a considerable improvement over the existing data in the mass range 10–60  $\text{MeV}/c^2$ .

### 3.3. Prospects for the $K^+ \rightarrow \pi^+ \nu \bar{\nu}$ Decay Study in the NA62 Experiment.

NA62 is a kaon decay in flight experiment at the CERN SPS. Its primary aim is to measure the branching ratio of the ultrarare decay  $K^+ \rightarrow \pi^+ \nu \bar{\nu}$  (expected branching ratio is of the order of  $10^{-10}$ ) with 10% precision by collecting about 100 signal events [5].

This decay is a Flavour Changing Neutral Current process, which in the Standard Model is forbidden at tree level. The hadronic matrix element entering the decay amplitude can be determined from semileptonic data. As a result, for this decay there is a theoretically clean dependence of probability on the CKM matrix elements  $V_{ts} \cdot V_{td}$ . Due to suppression in the framework of the Standard Model the  $K^+ \rightarrow \pi^+ \nu \bar{\nu}$  decay is a very sensitive probe of new physics.

The current experimental status of this decay is defined by the E787 and E949 experiments at BNL. Both experiments identified  $K^+ \rightarrow \pi^+ \nu \bar{\nu}$  decays by detecting the outgoing pion from kaon decays at rest. They have registered a combined total of seven events, which leads to the branching ratio measurement  $\text{BR}(K^+ \rightarrow \pi^+ \nu \bar{\nu}) = 1.73_{-1.05}^{+1.15} \cdot 10^{-10}$  [96].

Large statistics in NA62 will be achieved by using a high-intensity kaon beam. Protons from SPS beam will produce a secondary positively charged beam with a central momentum of 75  $\text{GeV}/c$ , consisting of kaons, protons, and pions. The total beam rate will be 750 MHz, resulting in  $4.5 \cdot 10^{12}$   $K^+$  decays per year.

The signal signature is a single  $K^+$  upstream matched with a single positive track downstream and no other particles detected. Most backgrounds to the signal decay come from other kaon decays with similar decay signatures when one or more of the decay products is misidentified or not detected. Experimental strategy combines high-resolution particle tracking and momentum measurement with particle identification in order to achieve a signal/background ratio of the order of 10.

Accidental coinciding of decay products with another beam kaon will be suppressed by tagging the kaon before it decays. Kinematical background suppression is based on the different missing mass  $m_{\text{miss}}^2 = (p_K - p_\pi)^2$  distributions of signal and background modes. It requires a good momentum resolution both for charged kaon and for outgoing charged pion.

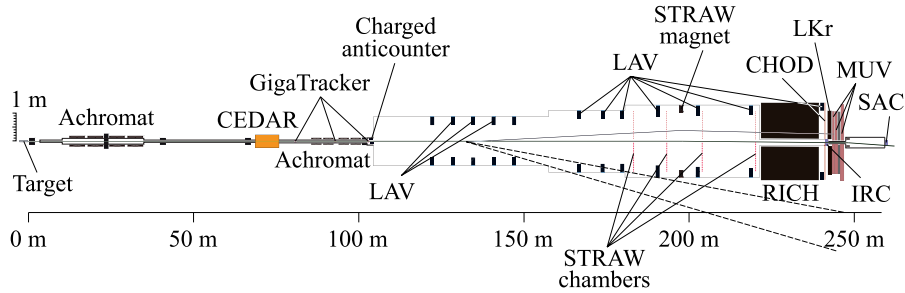


Fig. 16. The NA62 detector layout (from [97]). See the text for notations

The NA62 setup (Fig. 16) is using  $K^+$  decaying in flight from the unseparated  $(75 \pm 1)$  GeV/ $c$  charged beam. The 65-m-long decay volume is contained in a vacuum in order to keep the scattering-related background below the level of 1 event/year.

GigaTracker spectrometer based on silicon pixel detectors is used to measure the kaon momentum and direction with a resolution of  $\sigma(p)/p = 0.2\%$  and  $\sigma(\theta) = 16 \mu\text{rad}$ .

Straw tracker (STRAW in Fig. 16) made of four straw chambers and a dipole magnet providing the transverse momentum kick of  $p_t = 270$  MeV/ $c$  is used to measure the decay charged products momenta and position in space. Its expected momentum resolution is  $\sigma(p)/p = ((0.32 \oplus 0.008)p)\%$ .

The CEDAR, a Cherenkov differential counter, is used to identify kaons in the unseparated beam with 95% efficiency and time resolution below 100 ps at a rate of 45 MHz. Charged hodoscope CHOD will be used for triggering. Muon veto system (MUV) made of iron-scintillator calorimeters will veto  $K^+ \rightarrow \mu^+\nu$  decays at the  $10^5$  rejection level.

RICH is a ring-imaging Cherenkov counter that is used to provide an additional  $\pi-\mu$  separation and for the additional pion time measurement.

The photon veto system will reduce the background caused by many kaon decay modes, including the dominating  $\pi^+\pi^0$  decay. The requirement on the  $\pi^+$  momentum  $p < 35$  GeV/ $c$  guarantees the final-state gamma quanta total energy of about 40 GeV. Three groups of veto detectors will provide an angular coverage up to 50 mrad: the Large Angle Vetoes (LAV) made of rings of lead-glass blocks, LKr electromagnetic calorimeter and the small angle vetoes system that consists of the intermediate ring calorimeter (IRC) and the small-angle calorimeter (SAC).

All the detector elements implemented together should guarantee the rejection factor for generic kaon decays of the order of  $10^{12}$ , as well as the possibility to measure efficiencies and background suppression factors directly from the data.

## CONCLUSIONS

Even in the modern era of high-energy colliders the physics of kaon decays working on the particle physics intensity frontier is one of the most important sources of new knowledge on the fundamental properties of Nature.

## REFERENCES

1. *Fanti V. et al. (NA48 Collab.)*. The Beam and Detector for the NA48 Neutral Kaon CP Violations Experiment at CERN // Nucl. Instr. Meth. A. 2007. V. 574. P. 433–471.
2. *Batley R. et al. (NA48/1 Collab.)*. A High Sensitivity Investigation of  $K_S$  and Neutral Hyperon Decays Using a Modified  $K_S$  Beam (Addendum 2 to P253). CERN/SPSC 2000-002. 1999.
3. *Batley R. et al. (NA48/2 Collab.)*. Precision Measurement of Charged Kaon Decay Parameters with an Extended NA48 Setup (Addendum 3 to Proposal P253/CERN/SPSC). CERN-SPSC-2000-003. 1999.
4. *Lazzeroni C. et al. (NA62 Collab.)*. Precision Measurement of the Ratio of the Charged Kaon Leptonic Decay Rates // Phys. Lett. B. 2013. V. 719. P. 326–336.
5. *Anelli G. et al. (NA62 Collab.)*. Proposal to Measure the Rare Decay  $K^+ \rightarrow \pi^+ \nu \bar{\nu}$  at the CERN SPS. CERN-SPSC-2005-013. 2005.
6. *Lai A. et al. (NA48 Collab.)*. A Precise Measurement of the Direct CP Violation Parameter  $\text{Re}(\epsilon'/\epsilon)$  // Eur. Phys. J. C. 2001. V. 22. P. 231–254.
7. *Batley J.R. et al. (NA48/2 Collab.)*. Search for Direct CP-Violation in  $K^\pm \rightarrow \pi^\pm \pi^0 \pi^0$  Decays // Phys. Lett. B. 2006. V. 638. P. 22–29; Erratum // Ibid. V. 640. P. 297.
8. *Batley J.R. et al. (NA48/2 Collab.)*. Search for Direct CP Violating Charge Asymmetries in  $K^\pm \rightarrow \pi^\pm \pi^+ \pi^-$  and  $K^\pm \rightarrow \pi^\pm \pi^0 \pi^0$  Decays // Eur. Phys. J. C. 2007. V. 52. P. 875–891.
9. *Christenson J.H. et al.* Evidence for the  $2\pi$  Decay of the  $K(2)0$  Meson // Phys. Rev. Lett. 1964. V. 13. P. 138–140.
10. *Lai A. et al. (NA48 Collab.)*. Measurement of the Ratio  $\Gamma(K_L \rightarrow \pi^+ \pi^-)/\Gamma(K_L \rightarrow \pi^\pm e^\mp \nu)$  and Extraction of the CP Violation Parameter  $|\eta_{+-}|$  // Phys. Lett. B. 2007. V. 645. P. 26–35.
11. *Eidelman S. et al. (Particle Data Group)*. Review of Particle Physics // Phys. Lett. B. 2004. V. 592. P. 1–1109.
12. *Apostolakis A. et al. (CPLEAR Collab.)*. A Determination of the CP Violation Parameter  $\eta^\pm$  from the Decay of Strangeness Tagged Neutral Kaons // Phys. Lett. B. 1999. V. 458. P. 545.
13. *Alexopoulos T. et al. (KTeV Collab.)*. Measurements of  $K_L$  Branching Fractions and the CP Violation Parameter  $|\eta_{+-}|$  // Phys. Rev. D. 2004. V. 70. P. 092006.
14. *Ambrosino F. et al. (KLOE Collab.)*. Measurement of the Branching Ratio of the  $K_L \rightarrow \pi^+ \pi^-$  Decay with the KLOE Detector // Phys. Lett. B. 2006. V. 638. P. 140–145.

15. Olive K. A. *et al.* (*Particle Data Group*). Review of Particle Physics // *Chin. Phys. C*. 2014. V. 38. P. 090001.
16. Batley J. R. *et al.* (*NA48 Collab.*). A Precision Measurement of Direct CP Violation in the Decay of Neutral Kaons into Two Pions // *Phys. Lett. B*. 2002. V. 544. P. 97–112.
17. Abouzaid E. *et al.* (*KTeV Collab.*). Precise Measurements of Direct CP Violation, CPT Symmetry, and Other Parameters in the Neutral Kaon System // *Phys. Rev. D*. 2011. V. 83. P. 092001.
18. Gibbons L. K. *et al.* (*E731 Collab.*). Measurement of the CP Violation Parameter  $\text{Re}(\epsilon'/\epsilon)$  // *Phys. Rev. Lett.* 1993. V. 70. P. 1203.
19. Barr G. D. *et al.* (*NA31 Collab.*). A New Measurement of Direct CP Violation in the Neutral Kaon System // *Phys. Lett. B*. 1993. V. 317. P. 233.
20. Gamiz E., Prades J., Scimemi I. Charged Kaon  $K \rightarrow 3\pi$  CP Violating Asymmetries at NLO in CHPT // *JHEP*. 2003. V. 0310. P. 042.
21. Akopdzhanov G. A. *et al.* Measurements of the Charge Asymmetry of the Dalitz Plot Parameters for  $K^\pm \rightarrow \pi^\pm \pi^0 \pi^0$  Decays // *Eur. Phys. J. C*. 2005. V. 40. P. 343.
22. Batley J. R. *et al.* (*NA48/2 Collab.*). Measurement of the Dalitz Plot Slopes of the  $K^\pm \rightarrow \pi^\pm \pi^+ \pi^-$  Decay // *Phys. Lett. B*. 2007. V. 649. P. 349–358.
23. Colangelo G., Gasser J., Leutwyler H.  $\pi\pi$  Scattering // *Nucl. Phys. B*. 2001. V. 603. P. 125–179.
24. Batley J. R. *et al.* (*NA48/2 Collab.*). Observation of a Cusp-Like Structure in the  $\pi^0 \pi^0$  Invariant Mass Distribution from  $K^\pm \rightarrow \pi^\pm \pi^0 \pi^0$  Decay and Determination of the  $\pi\pi$  Scattering Lengths // *Phys. Lett. B*. 2006. V. 633. P. 173–182.
25. Budini P., Fonda L. Pion–Pion Interactions from Threshold Anomalies in  $K^+$  Decay // *Phys. Rev. Lett.* 1961. V. 6. P. 419–421.
26. Cabibbo N. Determination of the  $a_0 - a_2$  Pion Scattering Length from  $K^\pm \rightarrow \pi^\pm \pi^0 \pi^0$  Decay // *Phys. Rev. Lett.* 2004. V. 93. P. 121801.
27. Cabibbo N., Isidori G. Pion–Pion Scattering and the  $K \rightarrow 3\pi$  Decay Amplitudes // *JHEP*. 2005. V. 03. P. 021.
28. Colangelo G. *et al.* Cusps in  $K \rightarrow 3\pi$  Decays // *Phys. Lett. B*. 2006. V. 638. P. 187–194.
29. Bissegger M. *et al.* Radiative Corrections in  $K \rightarrow 3\pi$  Decays // *Nucl. Phys. B*. 2009. V. 806. P. 178–223.
30. Batley J. R. *et al.* (*NA48/2 Collab.*). Determination of the S-Wave  $\pi\pi$  Scattering Lengths from a Study of  $K^\pm \rightarrow \pi^\pm \pi^0 \pi^0$  Decays // *Eur. Phys. J. C*. 2009. V. 64. P. 589–608.
31. Adeva B. *et al.* (*DIRAC Collab.*). First Measurement of the  $\pi^+ \pi^-$  Atom Lifetime // *Phys. Lett. B*. 2005. V. 619. P. 50–60.
32. Batley J. R. *et al.* (*NA48/2 Collab.*). Empirical Parameterization of the  $K^\pm \rightarrow \pi^\pm \pi^0 \pi^0$  Decay Dalitz Plot // *Phys. Lett. B*. 2010. V. 686. P. 101–108.
33. Gevorkyan S. R., Tarasov A. V., Voskresenskaya O. Electromagnetic Effects in the  $K^+ \rightarrow \pi^+ \pi^0 \pi^0$  Decay // *Phys. Lett. B*. 2007. V. 649. P. 159.
34. Cabibbo N., Maksymowicz A. Angular Correlations in  $K_{e4}$  Decays and Determination of Low-Energy  $\pi-\pi$  Phase Shifts // *Phys. Rev.* 1965. V. 137. P. B438–B443; Erratum // *Phys. Rev.* 1968. V. 168. P. 1926.

35. Amoros G., Bijmens J. A Parametrization for  $K^+ \rightarrow \pi^+\pi^-e^+\nu$  // J. Phys. G. 1999. V. 25. P. 1607–1622.
36. Batley J.R. et al. (NA48/2 Collab.). Precise Tests of Low Energy QCD from  $K_{e4}$  Decay Properties // Eur. Phys. J. C. 2010. V. 70. P. 635–657.
37. Roy S.M. Exact Integral Equation for Pion–Pion Scattering Involving Only Physical Region Partial Waves // Phys. Lett. B. 1971. V. 36. P. 353.
38. Pislak S. et al. (BNL-E865 Collab.). High Statistics Measurement of  $K_{e4}$  Decay Properties // Phys. Rev. D. 2003. V. 67. P. 072004; Erratum // Phys. Rev. D. 2010. V. 81. P. 119903.
39. Rosselet L. et al. Experimental Study of 30,000  $K_{e4}$  Decays // Phys. Rev. D. 1977. V. 15. P. 574.
40. Pislak S. et al. (BNL-E865 Collab.). A New Measurement of  $K_{e4}^+$  Decay and the S Wave  $\pi\pi$  Scattering Length  $a_0^0$  // Phys. Rev. Lett. 2001. V. 87. P. 221801; Erratum // Phys. Rev. Lett. 2010. V. 105. P. 019901.
41. Batley J.R. et al. (NA48/2 Collab.). New Measurement of the Charged Kaon Semileptonic  $K^\pm \rightarrow \pi^+\pi^-e^\pm\nu$  ( $K_{e4}$ ) Decay Branching Ratio and Hadronic Form Factors // Phys. Lett. B. 2012. V. 715. P. 105–115; Addendum // Phys. Lett. B. 2015. V. 740. P. 364.
42. Beringer J. et al. (Particle Data Group). Review of Particle Physics // Phys. Rev. D. 2012. V. 86. P. 010001.
43. Brun R., Carminati F., Giani S. GEANT Detector Description and Simulation Tool. CERN-W5013. 1994.
44. Batley J.R. et al. (NA48/2 Collab.). Detailed Study of the  $K^\pm \rightarrow \pi^0\pi^0e^\pm\nu$  ( $K_{e4}^0$ ) Decay Properties // JHEP. 2014. V. 08. P. 159.
45. Barmin V.V. et al. Measurement of the Probability of the Decay  $K^+ \rightarrow \pi^0\pi^0e^+\nu$  // Sov. J. Nucl. Phys. 1988. V. 48. P. 1032.
46. Bolotov V.N. et al. Experimental Investigation of the Rare  $K^-$  Decay Modes  $K^- \rightarrow \pi^0\gamma e^-\bar{\nu}$  and  $K^- \rightarrow \pi^0\pi^0e^-\bar{\nu}$  // Sov. J. Nucl. Phys. 1986. V. 44. P. 68.
47. Gatti C. Monte Carlo Simulation for Radiative Kaon Decays // Eur. Phys. J. C. 2006. V. 45. P. 417–420.
48. Madigozhin D. High Precision Measurement of the Form Factors of the Semileptonic Decays  $K^\pm \rightarrow \pi^0l^\pm\nu(K_{l3})$  // PoS DIS2013. 2013. P. 135.
49. Alexopoulos T. et al. (KTeV Collab.). Measurements of Semileptonic  $K_L$  Decay Form-Factors // Phys. Rev. D. 2004. V. 70. P. 092007.
50. Ambrosino F. et al. (KLOE Collab.). Measurement of the  $K_L \rightarrow \pi\mu\nu$  Form-Factor Parameters with the KLOE Detector // JHEP. 2007. V. 0712. P. 105.
51. Yushchenko O.P. et al. (ISTRA+ Collab.). High Statistic Study of the  $K^- \rightarrow \pi^0\mu^-\nu$  Decay // Phys. Lett. B. 2004. V. 581. P. 31–38.
52. Yushchenko O.P. et al. (ISTRA+ Collab.). High Statistic Measurement of the  $K^- \rightarrow \pi^0e^-\nu$  Decay Form-Factors // Ibid. V. 589. P. 111–117.
53. Lai A. et al. (NA48 Collab.). Measurement of  $K_{\mu 3}^0$  Form Factors // Phys. Lett. B. 2007. V. 647. P. 341–350.

54. Antonelli M. et al. (*FlaviaNet Collab.*). An Evaluation of  $|V_{us}|$  and Precise Tests of the Standard Model from World Data on Leptonic and Semileptonic Kaon Decays // *Eur. Phys. J. C.* 2010. V. 69. P. 399–424.
55. Batley J.R. et al. (*NA48/2 Collab.*). Measurement of the Direct Emission and Interference Terms and Search for CP Violation in the Decay  $K^\pm \rightarrow \pi^\pm \pi^0 \gamma$  // *Ibid.* V. 68. P. 75–87.
56. Smith K.M. et al. A Search for CP Violation in  $K^\pm \rightarrow \pi^\pm \pi^0 \gamma$  Decays // *Nucl. Phys. B.* 1976. V. 109. P. 173–182.
57. Abrams R.J. et al. Test of CP Noninvariance in the Decay  $K^\pm \rightarrow \pi^\pm \pi^0 \gamma$  // *Phys. Rev. Lett.* 1973. V. 30. P. 500; 678.
58. Batley J.R. et al. (*NA48/2 Collab.*). Precise Measurement of the  $K^\pm \rightarrow \pi^\pm e^+ e^-$  Decay // *Phys. Lett. B.* 2009. V. 677. P. 246–254.
59. Bloch P. et al. Observation of the  $K^+ \rightarrow \pi^+ e^+ e^-$  Decay // *Phys. Lett. B.* 1975. V. 56. P. 201.
60. Alliegro C. et al. Study of the Decay  $K^+ \rightarrow \pi^+ e^+ e^-$  // *Phys. Rev. Lett.* 1992. V. 68. P. 278.
61. Appel R. et al. (*E865 Collab.*). A New Measurement of the Properties of the Rare Decay  $K^+ \rightarrow \pi^+ e^+ e^-$  // *Phys. Rev. Lett.* 1999. V. 83. P. 4482.
62. Batley J.R. et al. (*NA48/2 Collab.*). New Measurement of the  $K^\pm \rightarrow \pi^\pm \mu^+ \mu^-$  Decay // *Phys. Lett. B.* 2011. V. 697. P. 107–115.
63. D'Ambrosio G. et al. The Decays  $K \rightarrow \pi l^+ l^-$  beyond Leading Order in the Chiral Expansion // *JHEP.* 1998. V. 08. P. 004.
64. Friot S., Greynat D., De Rafael E. Rare Kaon Decays Revisited // *Phys. Lett. B.* 2004. V. 595. P. 301–308.
65. Dubnickova A.Z. et al. Kaon Decay Probe of the Weak Static Interaction // *Phys. Part. Nucl. Lett.* 2008. V. 5. P. 76–84.
66. Lafferty G.D., Wyatt T.R. Where to Stick Your Data Points: The Treatment of Measurements within Wide Bins // *Nucl. Instr. Meth. A.* 1995. V. 355. P. 541–547.
67. Park H.K. et al. (*HyperCP Collab.*). Observation of the Decay  $K^- \rightarrow \pi^- \mu^+ \mu^-$  and Measurements of the Branching Ratios for  $K^\pm \rightarrow \pi^\pm \mu^+ \mu^-$  // *Phys. Rev. Lett.* 2002. V. 88. P. 111801.
68. Ma H. et al. (*E865 Collab.*). A New Measurement of the Rare Decay  $K^+ \rightarrow \pi^+ \mu^+ \mu^-$  // *Phys. Rev. Lett.* 2000. V. 84. P. 2580.
69. Adler S. et al. (*E787 Collab.*). Observation of the Decay  $K^+ \rightarrow \pi^+ \mu^+ \mu^-$  // *Phys. Rev. Lett.* 1997. V. 79. P. 4756.
70. Appel R. et al. (*BNL E865 Collab.*). Search for Lepton Flavor Violation in  $K^+$  Decays // *Phys. Rev. Lett.* 2000. V. 85. P. 2877.
71. Ecker G., Pich A., de Rafael E. Radiative Kaon Decays and CP Violation in Chiral Perturbation Theory // *Nucl. Phys. B.* 1988. V. 303. P. 665.
72. Lazzeroni C. et al. (*NA62 Collab.*). Study of the  $K^\pm \rightarrow \pi^\pm \gamma \gamma$  Decay by the NA62 Experiment // *Phys. Lett. B.* 2014. V. 732. P. 65–74.
73. D'Ambrosio G., Portoles J. Unitarity and Vector Meson Contributions to  $K^+ \rightarrow \pi^+ \gamma \gamma$  // *Phys. Lett. B.* 1996. V. 386. P. 403–412; Erratum // *Phys. Lett. B.* 1997. V. 395. P. 389.

74. *Batley J. R. et al. (NA48/2 Collab.)*. A New Measurement of the  $K^\pm \rightarrow \pi^\pm \gamma \gamma$  Decay at the NA48/2 Experiment // *Phys. Lett. B*. 2014. V. 730. P. 141–148.
75. *Kitching P. et al. (E787 Collab.)*. Observation of the Decay  $K^+ \rightarrow \pi^+ \gamma \gamma$  // *Phys. Rev. Lett.* 1997. V. 79. P. 4079–4082.
76. *Cirigliano V., Rosell I.* Two-Loop Effective Theory Analysis of  $\pi(K) \rightarrow e\bar{\nu}_e[\gamma]$  Branching Ratios // *Phys. Rev. Lett.* 2007. V. 99. P. 231801.
77. *Masiero A., Paradisi P., Petronzio R.* Probing New Physics through  $\mu$ – $e$  Universality in  $K \rightarrow l\nu$  // *Phys. Rev. D*. 2006. V. 74. P. 011701.
78. *Masiero A., Paradisi P., Petronzio R.* Anatomy and Phenomenology of the Lepton Flavor Universality in SUSY Theories // *JHEP*. 2008. V. 11. P. 042.
79. *Ellis J., Lola S., Raidal M.* Supersymmetric Grand Unification and Lepton Universality in  $K \rightarrow l\nu$  Decays // *Nucl. Phys. B*. 2009. V. 812. P. 128–143.
80. *Kelner S. R., Kokoulin R. P., Petrukhin A. A.* Bremsstrahlung from Muons Scattered by Atomic Electrons // *Phys. At. Nucl.* 1997. V. 60. P. 576–583; *Yad. Fiz.* 1997. V. 60. P. 657.
81. *Ambrosino F. et al. (KLOE Collab.)*. Precise Measurement of  $\Gamma(K \rightarrow e\nu(\gamma))/\Gamma(K \rightarrow \mu\nu(\gamma))$  and Study of  $K \rightarrow e\nu\gamma$  // *Eur. Phys. J. C*. 2009. V. 64. P. 627; Erratum // *Eur. Phys. J.* 2010. V. 65. P. 703.
82. *Lacker H., Menzel A.* Simultaneous Extraction of the Fermi Constant and PMNS Matrix Elements in the Presence of a Fourth Generation // *JHEP*. 2010. V. 07. P. 006.
83. *Batley J. R. et al. (NA48/2 Collab.)*. Search for the Dark Photon in  $\pi^0$  Decays // *Phys. Lett. B*. 2015. V. 746. P. 178–185.
84. *Riordan E. M. et al. (SLAC E141 Collab.)*. A Search for Short Lived Axions in an Electron Beam Dump Experiment // *Phys. Rev. Lett.* 1987. V. 59. P. 755.
85. *Bross A. et al.* A Search for Short-Lived Particles Produced in an Electron Beam Dump // *Phys. Rev. Lett.* 1991. V. 67. P. 2942.
86. *Andreas S., Niebuhr C., Ringwald A.* New Limits on Hidden Photons from Past Electron Beam Dumps // *Phys. Rev. D*. 2012. V. 86. P. 095019.
87. *Babusci D. et al. (KLOE-2 Collab.)*. Limit on the Production of a Light Vector Gauge Boson in Phi Meson Decays with the KLOE Detector // *Phys. Lett. B*. 2013. V. 720. P. 111.
88. *Adlarson P. et al. (WASA-at-COSY Collab.)*. Search for a Dark Photon in the  $\pi^0 \rightarrow e^+e^-\gamma$  Decay // *Phys. Lett. B*. 2013. V. 726. P. 187.
89. *Agakishiev G. et al. (HADES Collab.)*. Searching a Dark Photon with HADES // *Phys. Lett. B*. 2014. V. 731. P. 265.
90. *Merkel H. et al. (A1 Collab.)*. Search at the Mainz Microtron for Light Massive Gauge Bosons Relevant for the Muon  $g-2$  Anomaly // *Phys. Rev. Lett.* 2014. V. 112. P. 221802.
91. *Abrahamyan S. et al. (APEX Collab.)*. Search for a New Gauge Boson in Electron–Nucleus Fixed-Target Scattering by the APEX Experiment // *Phys. Rev. Lett.* 2011. V. 107. P. 191804.
92. *Lees J. P. et al. (BaBar Collab.)*. Search for a Dark Photon in  $e^+e^-$  Collisions at BaBar // *Phys. Rev. Lett.* 2014. V. 113. P. 201801.

93. *Pospelov M.* Secluded  $U(1)$  below the Weak Scale // *Phys. Rev. D.* 2009. V. 80. P. 095002.
94. *Endo M., Hamaguchi K., Mishima G.* Constraints on Hidden Photon Models from Electron  $g-2$  and Hydrogen Spectroscopy // *Phys. Rev. D.* 2012. V. 86. P. 095029.
95. *Davoudiasl H., Lee H. S., Marciano W. J.* Muon  $g-2$ , Rare Kaon Decays, and Parity Violation from Dark Bosons // *Phys. Rev. D.* 2014. V. 89. P. 095006.
96. *Artamonov A. V. et al. (E949 Collab.).* New Measurement of the  $K^+ \rightarrow \pi^+ \nu \bar{\nu}$  Branching Ratio // *Phys. Rev. Lett.* 2008. V. 101. P. 191802.
97. *Massri K.* The NA62 Experiment at CERN; Prospects for the  $K^+ \rightarrow \pi^+ \nu \bar{\nu}$  Measurement // *PoS DIS2014.* 2014. P. 254.